Atmospheric Research 295 (2023) 107010

Contents lists available at ScienceDirect

Atmospheric Research

journal homepage: www.elsevier.com/locate/atmosres

Effects of the river breeze on the transport of gases in Central Amazonia

Flávio A.F. D'Oliveira [a,*], Cleo Q. Dias-Júnior [a,b], Julia C.P. Cohen [a,c], Dominick V. Spracklen [d], Edson P. Marques Filho [e], Paulo Artaxo [f]

[a] Environmental Science Graduate Program – PPGCA, Federal University of Pará (UFPA), Belém, PA, Brazil
[b] Department of Physics, Federal Institute of Pará (IFPA), Belém, PA, Brazil
[c] Faculty of Meteorology, Federal University of Pará (UFPA), Belém, PA, Brazil
[d] School of Earth and Environment, University of Leeds, Leeds, United Kingdom
[e] Interdisciplinary Center for Energy and Environment, Federal University of Bahia, Salvador, BA, Brazil
[f] Institute of Physics, University of São Paulo (USP), São Paulo, SP, Brazil

ARTICLE INFO

Keywords:
Amazonia
River breeze
Gas transport
Recirculation zones

ABSTRACT

River breezes occur regularly along the Amazonia river but little is known about their effects on air pollution. During the first week of August 2014, river breeze events were observed on two days on the banks of the Negro River, central Amazonia. The WRF-Chem model was used to analyze this period to understand the formation mechanism and the influence of the river breeze on the transport of pollutants such as ozone (O_3) and carbon monoxide (CO). We show that the river breeze occurred due to a reduction of the easterly winds associated with the cooling of the waters of the Negro River. The river breeze was responsible for inhibiting the transport of pollutants to the East, increasing its concentrations while breeze circulation is observed, as well as a re-circulation of these gases on the riverbank where the breeze was associated. The strongest breeze occurred in a forest region which maintained the highest concentrations of CO and O_3 on the East bank of the Negro River. In the Urban region, the breeze was less intense and had a shorter duration, however, it was still able to maintain higher concentrations of CO and O_3 in the western region of the city of Manaus, which is a predominantly residential region and therefore, the population of this region lives in a more polluted environment during the occurrence of breezes.

1. Introduction

The Amazonian rainforest region is one of the largest areas of tropical forest on the planet (Lapola et al., 2008), it has great a biodiversity and is one of the main sources of heat and humidity in the tropics, playing an important role in the local, regional and global climate system (Shukla et al., 1990; Werth and Avissar, 2002; Malhi et al., 2008; Cheng et al., 2013). In addition to its extensive forest area, it has the largest hydrographic basin in the world, made up of large rivers such as Negro, Solimões, Amazonas, Tapajós and Xingu. These rivers play a fundamental role in the hydrological cycle (Marengo, 2005). Several studies have shown the formation of a local circulation, known as a river breeze, in these rivers (Pereira Oliveira and Fitzjarrald, 1993; Silva Dias et al., 2004; Lu et al., 2005; Cohen et al., 2014; Matos and Cohen, 2016; Corrêa et al., 2021), which impact the distribution of precipitation, carbon dioxide (CO_2) fluxes, the formation of low-level jets, among others.

The river breeze is a type of local circulation that occurs due to the thermal contrast of large water bodies of rivers and an adjacent area with different characteristics (eg forest, city, pasture), and is observed in several places in the world (Zhong et al., 1991; Pereira Oliveira and Fitzjarrald, 1993; Hrebtov and Hanjalić, 2019; Jiang et al., 2021). The formation mechanism of the river breeze circulation is similar to that observed for the sea breeze, that is, they occur due to the temperature gradient generated by the different thermal capacities of the two different surfaces. During the day time, the land surface heats up faster than the water, which induces the formation of a circulation, bringing the less warm and humid air over the river towards the land surface.

The city of Manaus is the largest metropolis in the northern region of Brazil, with a population of 2.255.903 inhabitants (IBGE, 2022) and a vehicle fleet of 855.9 thousand vehicles in 2021 (DETRAN, 2022). The city, located on the left bank of the Negro River, is home to the Industrial Pole of Manaus (IPM), with >500 industries established in various segments such as electronics, automobile, shipbuilding, mechanics, etc.

* Corresponding author.
E-mail address: flavio.doliveira@ig.ufpa.br (F.A.F. D'Oliveira).

https://doi.org/10.1016/j.atmosres.2023.107010
Received 7 March 2023; Received in revised form 6 September 2023; Accepted 6 September 2023
Available online 12 September 2023

(SUFRAMA, 2022). All these elements combined form a large source of anthropogenic aerosol and gas emissions, within an area surrounded by forest and rivers. The effects of the urban area of Manaus on the chemical composition of the atmosphere have been the focus of several studies related to the formation of secondary aerosols and the transport of the plume of pollutants from the urban area to other regions (Kuhn et al., 2010; Trebs et al., 2012; Cirino et al., 2018; Shrivastava et al., 2019).

Carbon monoxide (CO) is a colorless and odorless gas generated by the incomplete burning of fuels that contain carbon in their composition. With an average lifetime of approximately one month and has a high concentration close to the surface, it is an excellent tracer of anthropogenic pollution sources, such as those generated by industries, motor vehicles and forest fires. Several studies show an increase in CO emission during the dry season in the Amazonia region (Torres et al., 2010; Andreae et al., 2012; Vasconcelos et al., 2015; Santos et al., 2017; Moraes et al., 2022), and this may have many undesirable effects on the health of the population. When inhaled, CO is absorbed by the lungs and transported to the bloodstream, and its affinity for binding to hemoglobin is 200 times greater than oxygen, forming what is known as carboxyhemoglobin (COHb) (Bleecker, 2015). It needs to be reiterated, however, that air pollution is a complex mixture of heterogeneous gaseous and particulate pollutants that can affect human health (Block et al., 2012), and CO is rarely found at high concentrations in outdoors environments, but there are studies showing a concern on low level CO concentrations impacts on human health and positive association of daily mortality with short-term exposure to ambient CO at levels below the current air quality guidelines (Townsend and Maynard, 2002; Levy, 2015; Chen et al., 2021), in addition to CO being a precursor of ozone (O_3).

The O_3 is a gas that is naturally present in the stratosphere and plays a vital role for life on the planet against the action of ultraviolet radiation from the Sun. In the troposphere, this gas is classified as a secondary pollutant because it is not emitted directly, but is formed through chemical reactions of oxidant precursors. There are several precursors of O_3 such as nitrogen oxides (NO_x), CO, methane, among others (Parrish and Fehsenfeld, 2000; Yue and Unger, 2014). In plants, its absorption occurs through stomatal uptake, but impairs photosynthesis, reduces plant growth and biomass accumulation, limits crop productivity, and affects stomatal control over plant transpiration of water vapor between the surface of the leaf and the atmosphere (Avnery et al., 2011; Ainsworth et al., 2012; Hollaway et al., 2012; Yue and Unger, 2014, 2018). In animals, its main form of absorption is through inhalation, being absorbed by the respiratory tract and conducted to the bloodstream (Bush et al., 1996; Sarangapani et al., 2003). Studies show evidence of the effects of exposure to this gas on human health, such as difficulty breathing, inflammation of the airways, premature deaths, obesity, increased admissions to psychiatric emergencies, among others (Koman and Mancuso, 2017; Nuvolone et al., 2018; Zhang et al., 2019; Bernardini et al., 2020; Grulke and Heath, 2020).

The city of Manaus is one of the sources of O_3 in the central Amazonia region due to its industrial activity and the intense circulation of motor vehicles, which causes a great contrast with the large area of surrounding forest (Kuhn et al., 2010). It is also known that this gas can be transported by downdrafts to the surface (Betts et al., 2002; Dias-Junior et al., 2017; Melo et al., 2019; D'Oliveira et al., 2022), in addition to to have its concentration increased during biomass burning (Crutzen and Andreae, 1990; Bourgeois et al., 2021).

Studies on the influence of breeze circulations on pollution of coastal cities have already been carried out in several locations, showing their impacts on the transport of O_3 and aerosols in cities of the northern hemisphere (Boyouk et al., 2011; Monteiro et al., 2016; Li et al., 2020) and also in the Amazonia (Trebs et al., 2012; Zhao et al., 2021).

However, recently the numbers of forest fires in the Amazonia have shown a significant increase (Barlow et al., 2020; Cano-Crespo et al., 2021; Silveira et al., 2022). In addition, the urban area of Manaus also showed an increase of population and in the vehicle fleet. In this context, it is necessary to assess how local circulations can influence the transport of these anthropogenic pollutants. Therefore, this work aims to study the effect of river breeze circulations on the transport of gaseous air pollutants (CO and O_3) in the central Amazonia region. We seek to better understand, through simulations with WRF-Chem, the mechanism of formation of these breezes and how they can alter the transport of these gases.

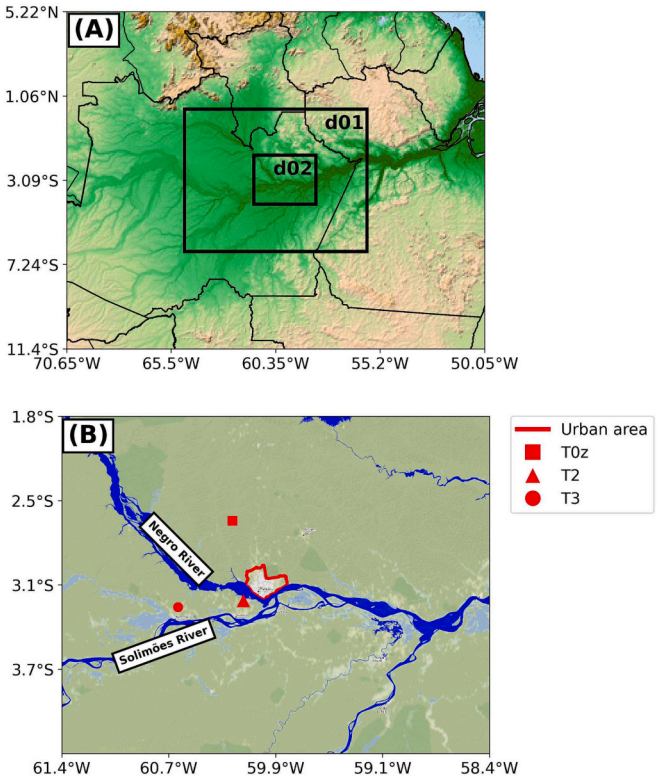

Fig. 1. (A) WRF-Chem domains used in this work. Domain d01 has 10 km of horizontal resolution and domain d02 has 2 km. (B) Location of experimental sites, urban area of Manaus and rivers in the study region.

2. Material and methods

In this work, the WRF-Chem model was used to simulate the atmospheric flow for the first four days of August 2014 (between the 1st and 5th), over the Manaus region, in central Amazonia. To verify the predictions generated by the model, measurements collected during the experimental campaigns of the GoAmazon 2014/5 project were used in three different sites (T0z, T2 and T3) located in the surroundings of Manaus (Fig. 1B). The description of the study area, experimental sites, collected data and numerical experiment design are detailed below.

2.1. Study area and experimental data

The city of Manaus is located in the central Amazonia region, more precisely at the confluence of the Negro and Solimões rivers (Fig. 1B). With 377 km^2 of urbanized area, inserted in a territorial extension of 11,401.092 km^2, it has an estimated population of 2,255,903 inhabitants (IBGE, 2022). This region is characterized by presenting an important contrast of atmospheric constituents between the polluted urban area and the surrounding natural environments, with more pristine air conditions. For this reason, this region was studied in the GoAmazon 2014/5 experiment (Martin et al., 2016).

The experimental data used in this work were collected at three different experimental sites: T0z (2.5946° S, 60.2093° W); T2 (3.1392°

Table 1
Description of the instruments used in the experimental sites of the GoAmazon 2014/5 project to collect gases (CO and O_3) and meteorological data.

Experimental Sites	Measured Variables	Sensors	Sample Rate	Height
T0z	CO	Picarro Model G130	5 min	38.75 m
	O_3	Thermo 49i-TSi	5 min	38.75 m
	Temperature	PT-100	5 min	51.1 m
	Precipitation	EM ARG-100	30 min	51.35 m
	Wind Speed and Direction	Vector W200P/ Vector A100R	30 min	51.9/ 51.45 m
T2	CO	LGR ICOS N2O/ CO-23D	5 min	2 m
	O_3	Thermo 49i-TSi	5 min	2 m
	Temperature	U30 Station	5 min	2 m
	Precipitation	GSM-UDP (HOBO)	5 min	2 m
	Wind Speed and Direction	Lufft WS800-UMB	5 min	2 m
T3	CO	Picarro CRDS G2401 analyzer	5 min	10 m
	O_3	Thermo 49i-TSi	5 min	10 m
	Temperature	WTX520 (Vaisala)	1 s	10 m
	Precipitation	WTX520 (Vaisala)	1 s	10 m
	Wind Speed and Direction	WTX520 (Vaisala)	1 s	10 m

Table 2
WRF-Chem configurations used.

WRF-Chem Configurations		
Domains	d01	d02
Points along x coordinate	111	171
Points along y coordinate	80	135
Vertical levels	60	60
Grid resolution	10 km	2 km
Physical Options		
Longwave radiation	RRTMG	
Shortwave radiation	RRTMG	
Surface layer	MYNN Scheme	
Land-surface model	NOAH Surface model	
Boundary layer scheme	MYNN 2.5	
Microphysics	Morrison 2-Moment	
Chemical Options		
Chemistry option	Mozart with MOSAIC aerosols	
Photolysis option	New TUV	

S, 60.1315° W); and T3 (3.2133° S, 60.5987° W). T0z is located in the central Amazonia Basin, 60 km NNW of downtown Manaus and 40 km from the metropolis margins. It is within a pristine *terra firme* rainforest in the *Reserva Biológica do Cuieiras* (Martin et al., 2010). T2 site is located at Hotel Tiwa, that is surrounded by a forest and adjacent to the river (Negro River) with river width of 7.5 to 11.7 km, and just downwind of Manaus, depending on direction of prevailing winds. The T3 site is located 70 km downwind of Manaus. It is a pasture site of 2.5 km by 2 km in size. The information collected and the instruments used in each of the experimental sites are presented in Table 1. For more detailed information about the collected data and the experimental methodology employed, please see Martin et al. (2016).

2.2. Model description and experimental design

Numerical simulations of atmospheric flow were performed with the WRF-Chem model in version 4.2 (Grell et al., 2005). The settings and the main physical and chemical options used in our simulations are shown in Table 2, with the cumulus parameterization turned off in the two domains used in this work. The arrangement of the model's domains is shown in Fig. 1A.

The initial and boundary conditions for chemical and atmospheric aerosols were taken from CAM-Chem (Lamarque et al., 2012). The initial and boundary conditions for meteorological variables were taken from the reanalysis of the European Centre for Medium-Range Weather Forecasts (ECMWF) ERA5 global reanalysis (Hersbach et al., 2020), with spatiotemporal resolutions of 0.25° in the horizontal direction and 6 h, respectively.

For anthropogenic emissions, information from the EDGAR-HTAP database (Emissions Database for Global Atmospheric Research with Task Force on Hemispheric Transport of Air Pollution) in version 2.2, was used. This information is representative of the year 2010, with a horizontal resolution of 0.1° x 0.1° (Janssens-Maenhout et al., 2019). Due to the lack of information on anthropogenic emissions in the Amazonia, some studies have carried out their own local emissions inventories to better represent the chemistry of the atmosphere in the central Amazonia region (Rafee et al., 2017; Medeiros et al., 2017; D'Oliveira et al., 2022). In this work, road transport and electricity emissions from EDGAR-HTAP were modified according to local emissions estimates obtained from the VEIN (Vehicle Emissions Inventory) model, version 0.9.13 (Ibarra-Espinosa et al., 2018) only in the domain d02. VEIN is a bottom-up model used to obtain high-resolution vehicle emissions inventories. The thermoelectric emissions, the type of fuel and its monthly consumption were provided by the brazilian electric power generation company ELETROBRAS (ELETROBRÁS, 2014). Gas emissions were entered in the d02 domain of the model as categories "POW" for energy emissions and "TRA" for transport emissions.

For the biogenic emissions, we used the Model of Emissions of Gases and Aerosols from Nature (MEGAN) version 2 (Guenther et al., 2006). These emissions were calculated online based on driving variables such as ambient temperature, solar radiation, leaf area index and plant functional types, this model estimates the net terrestrial biosphere emission rates for different trace gases and aerosols with a global coverage of approximately 1 km^2 spatial resolution.

For emissions from biomass burning, NCAR's Fire Inventories (FINN), version 1.5 (Wiedinmyer et al., 2011) was used. The FINN data comprises a daily estimate with grid spacing of 1 km2 based on the location and time of active fires detected by the product of thermal and fire anomalies from the MODIS satellite (Giglio et al., 2003). FINN data offers global coverage, high temporal and spatial resolution and includes emissions for a large number of chemical species including CO_2, CO, NO_x, NH_3, CH_4 volatile and semi-volatile organic compounds (VOCs and SMVOCs), black carbon (BC) and aerosols of organic carbon (OC). FINN emissions are incremented into the WRF-Chem using a diurnal cycle that peaks in the early afternoon (local time) based on Giglio (2007), and then injection of the emissions into the grid in the model is evenly distributed across the atmospheric boundary layer (Dentener et al., 2006), as shown by the analysis of plume heights over the Amazonia region (Marenco et al., 2016; Gonzalez-Alonso et al., 2019). FINN has been widely used in studies using atmospheric chemical transport models to simulate changes in air quality from local to global scale (Xu et al., 2018; Ghude et al., 2020; Faulstich et al., 2022; D'Oliveira et al., 2022).

The model integration time was 120 h, in the period from 00:00 UTC on July 31th, 2014 to 00:00 UTC on August 5th, 2014, the first 24 h being used as spin up. In this period, the analyzes of the accumulated precipitation in the three experimental sites (Fig. 2) show the occurrence of precipitation only on the 4th of August: at 20:00 UTC in the T3 site (26.56 mm in the total accumulated); and at 21:00 UTC at the T0z site (0.5 mm in cumulative total). No precipitation was observed at T2 site. These days are part of the dry period in central Amazonia (Marengo et al., 2001), ideal for studying the effects of anthropogenic emissions and also because it is the period when river breezes are most evident (Planchon et al., 2006).

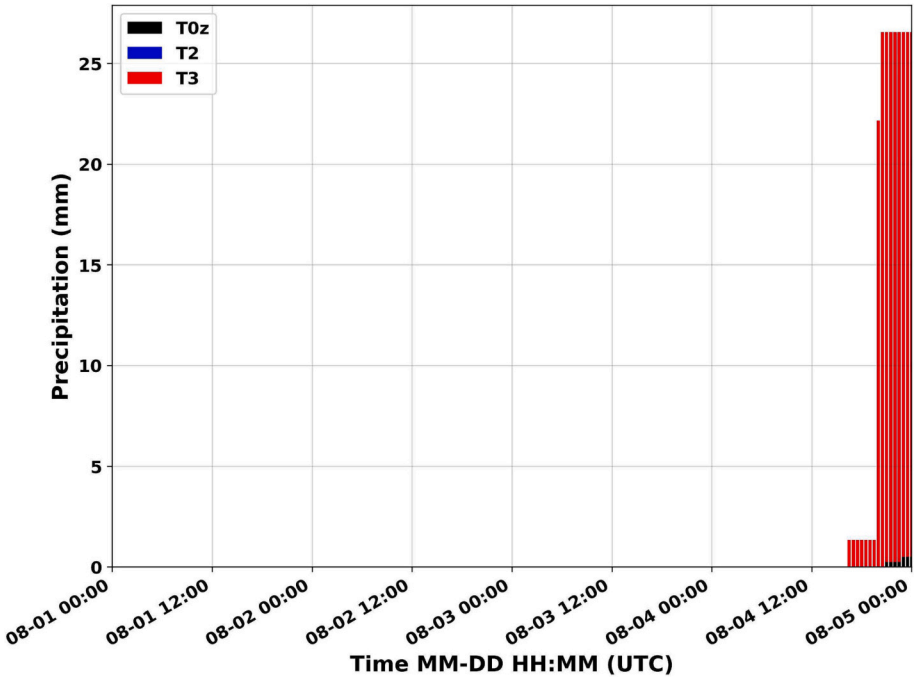

Fig. 2. Accumulated precipitation in mm at the experimental sites T0z, T2 and T3 of the GoAmazon project, during the study period.

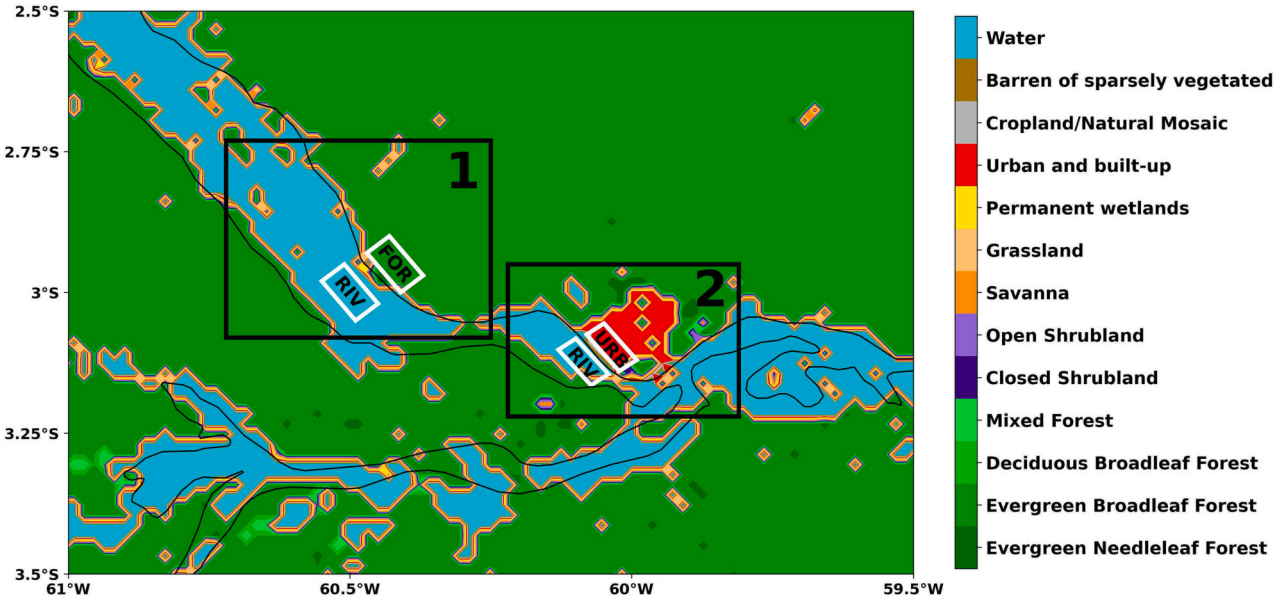

Fig. 3. Classification of land use obtained through MODIS Land Cover Type Data Product (MCD12Q1) and classification of the International Geosphere-Biosphere Program (IGBP) and the geographic location of the analyzed areas in: (1) Forest; and (2) Urban.

2.3. Identification of the river breeze

The criterion adopted in this work to identify a breeze circulation will be based on the diurnal change in surface wind direction in the opposite direction to the original direction (Borne et al., 1998; Furberg et al., 2002). It is known that the predominant wind direction in the Amazonia region is the easterlies winds (Pereira Oliveira and Fitzjarrald, 1993; Silva Dias et al., 2004; Lu et al., 2005; Santos et al., 2014; Germano et al., 2017; Corrêa et al., 2021; Zhao et al., 2021). Depending on the location where we are looking for the breeze signal, the breeze can be seen by changing the wind direction, but also in the weakening or intensifying of these winds (Germano et al., 2017; Corrêa et al., 2021). Our intention is just looking when these winds are in the opposite direction from the easterlies. This criterion was adopted due to the interest of verifying how the change in the predominant wind direction can alter the dynamics of gas transport in the region. In this work, the temperature gradient between river and forest and river and urban was obtained as follows: We calculated the average air temperature at 2 m from the surface for the four areas indicated in the rectangles of Fig. 3. The temperature gradients (ΔT) between river and forest and between river and urban were obtained through the difference between the average air temperatures in the rectangles FOR and RIV (square 1) and URB and RIV (square 2).

River breeze analyzes was carried out in two different areas (Fig. 3).

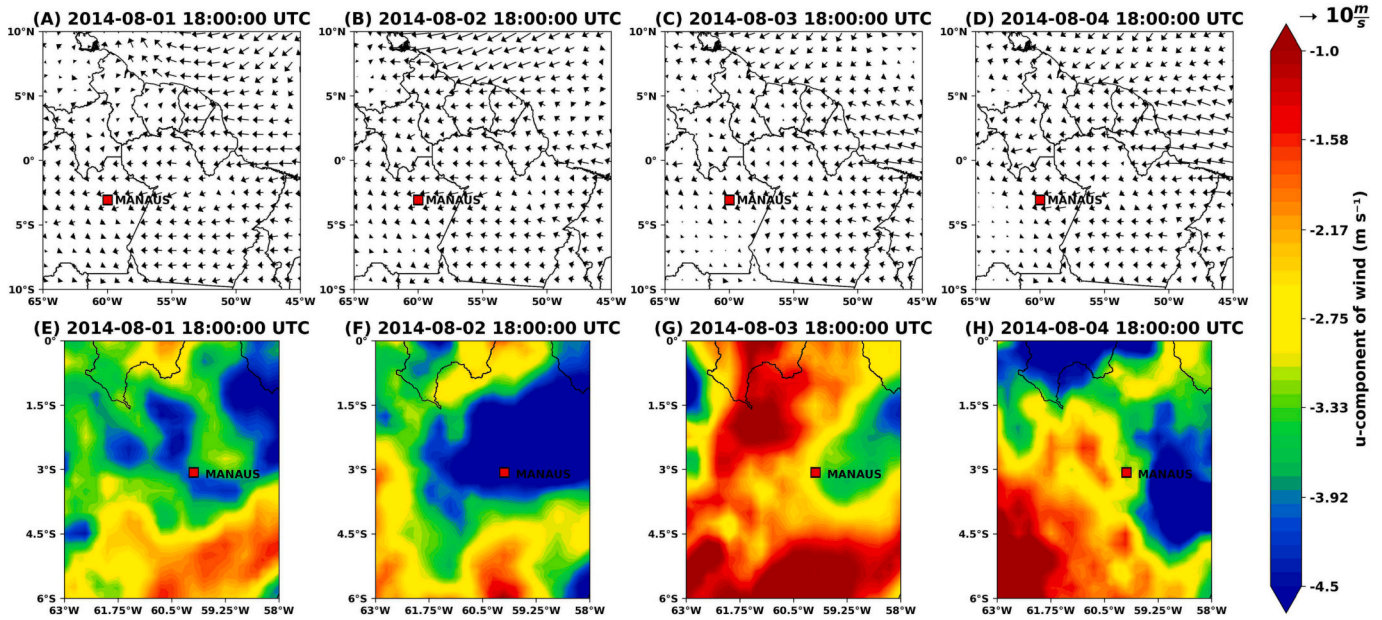

Fig. 4. Horizontal wind (arrows, m s^{-1}) and zonal wind (shaded, m s^{-1}) at 925 hPa from ERA5 reanalysis between 1st and 4th August 2014: (A) and (E) 18:00 UTC of the 1st of August; (B) and (F) 18:00 UTC on the 2nd of August; (C) and (G) 18:00 UTC on 3rd August; and (D) and (H) 18:00 UTC on 4th August.

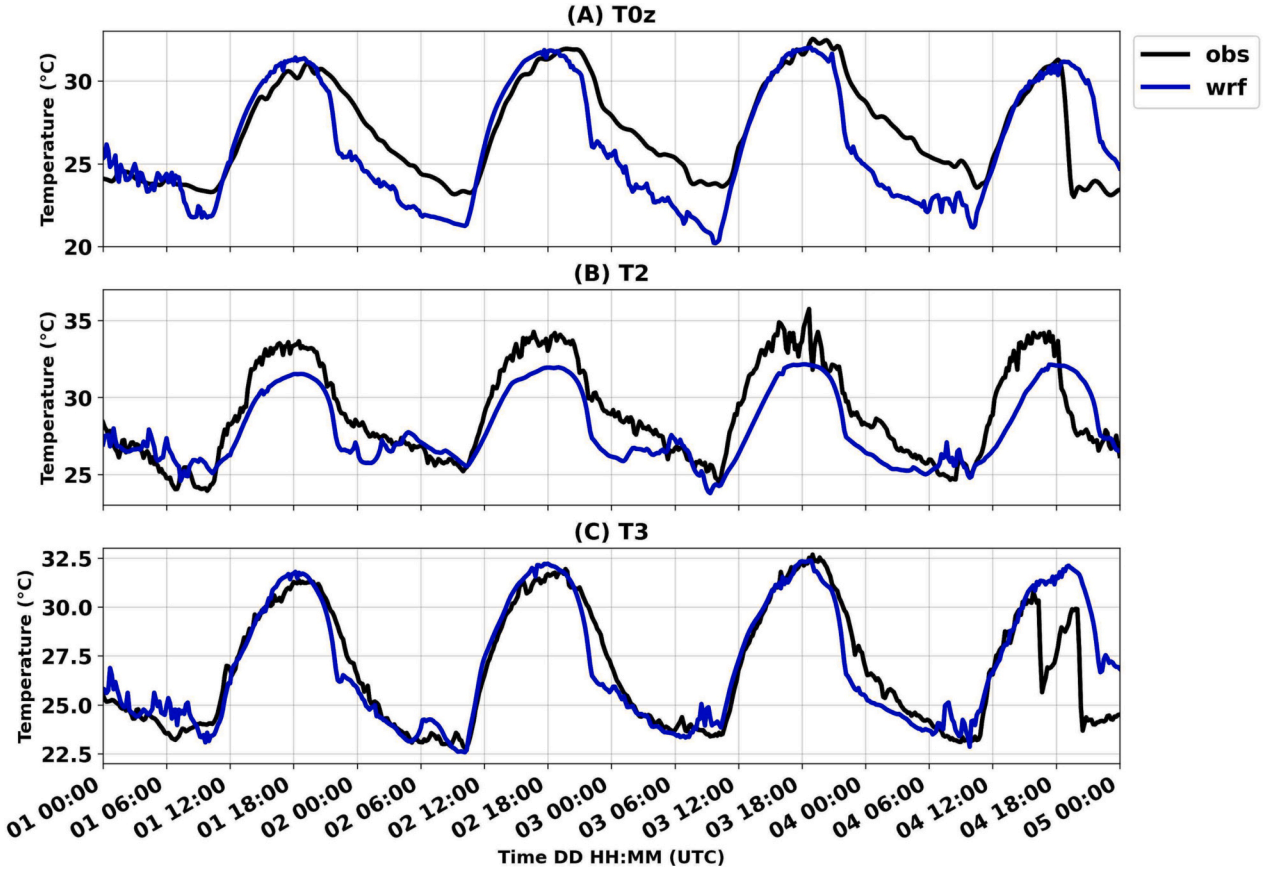

Fig. 5. Air temperature at sites (A) T0z, (B) T2 and (C) T3. The solid black line represents the experimental data and the solid blue line the simulation data with the WRF at 2 m. (For interpretation of the references to colour in this figure legend, the reader is referred to the web version of this article.)

Area 1 with a predominance of forest land cover on the banks of the Negro River (called "Forest") and area 2, with the contrast between the urban region of Manaus and the Negro River (called "Urban"). The reason of these two areas was chosen results from previous analyzes of the wind field, which show the presence of river breeze circulation in places with different land cover characteristics, in addition to the different position in relation to the Negro River. Furthermore, a separate analysis for the city is important, as it will be possible to investigate the

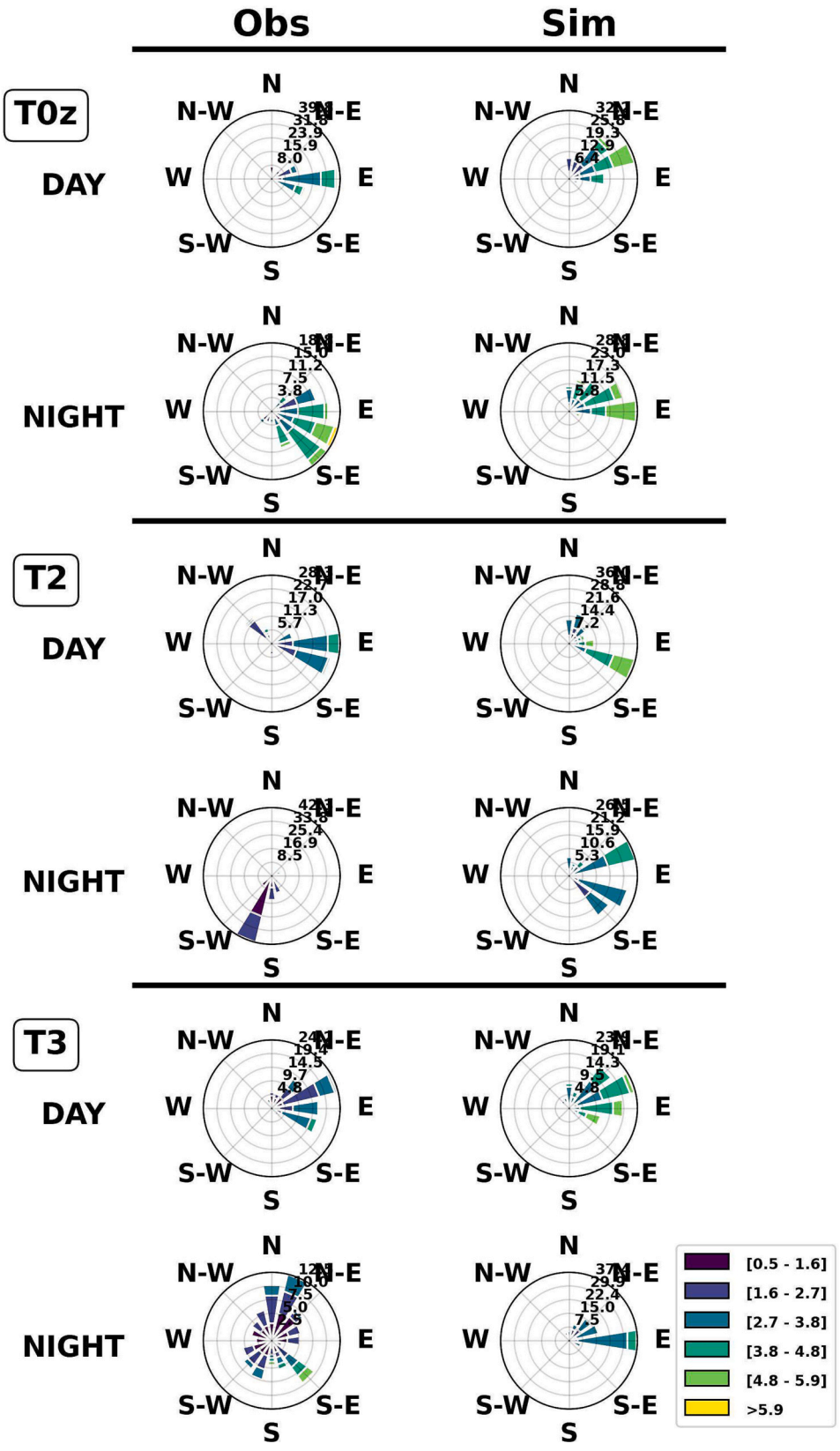

Fig. 6. Comparison of the wind rose data from the experimental sites for the observed data (Obs) on the left, and simulated (Sim) on the right, during the entire simulation period separated into day and night. The colors represent the wind speed in m s^{-1}. (For interpretation of the references to colour in this figure legend, the reader is referred to the web version of this article.)

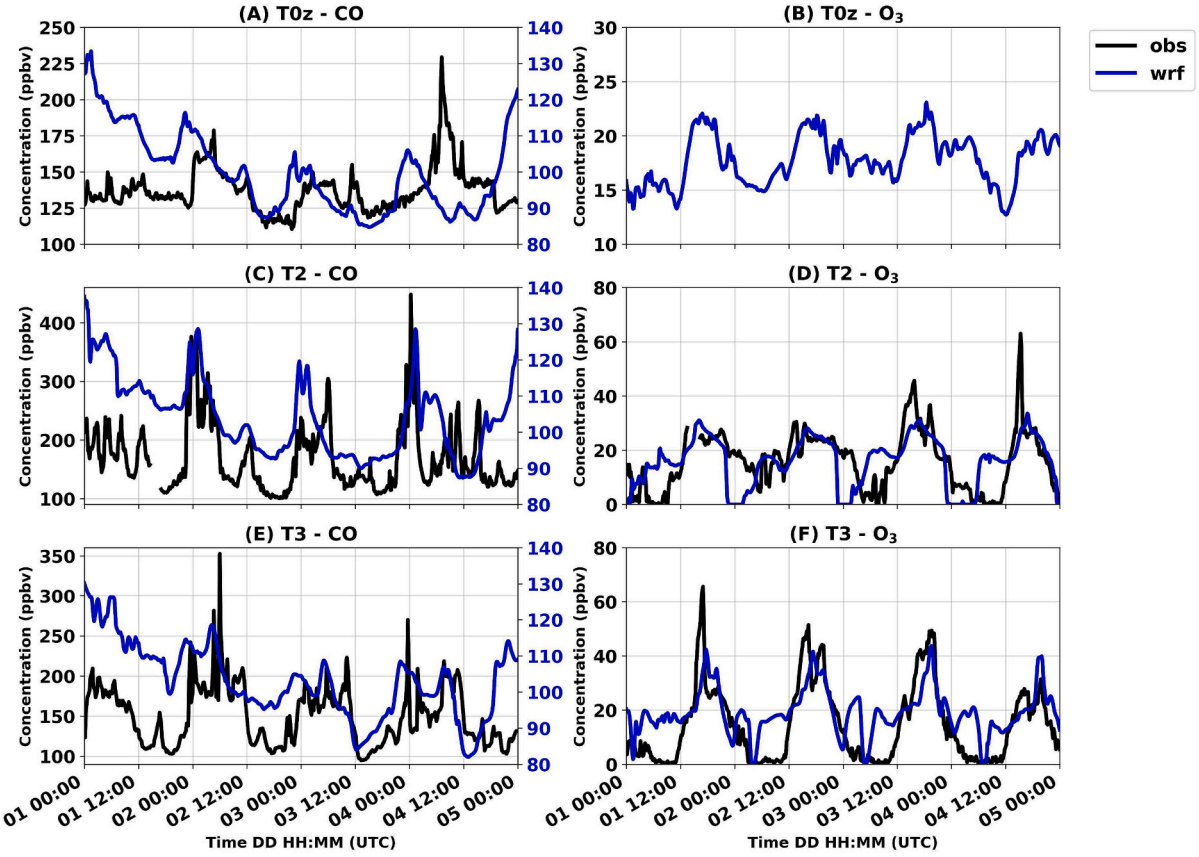

Fig. 7. CO and O_3 concentration measured and simulated at the level closest to the surface in experimental sites T0z, T2 and T3. The black line represents the collected data and the blue line the WRF-Chem simulation data. (For interpretation of the references to colour in this figure legend, the reader is referred to the web version of this article.)

impact of urbanization on local circulation and, consequently, on the quality of life of the population.

3. Results and discussion

3.1. Large scale analysis and validation of the simulation

Analysis of large-scale wind field is important as it affects the development of breeze circulation (Bechtold et al., 1991; Arritt, 1993). For example, Silva Dias et al. (2004) observed that river breezes that occurred on the east bank of the Tapajós River (in central Amazonia) were associated with weaker easterly wind events caused by a phenomena called *friagem* (Camarinha-Neto et al., 2021). Another important example for the same region is showed by Lu et al. (2005), who observed no change in wind direction on the Tapajós River caused by river breezes during conditions of strong easterly winds. The analysis of large-scale winds is important to verify whether they exert any influence on the formation or intensification of the river breeze.

During the analyzed period, the ERA5 reanalysis data show that the large-scale wind field (925 hPa pressure level) is essentially from the east, with wind direction variations between northeast and east (Fig. 4). However, it was observed that on the 3rd and 4th of August there was a weakening of the zonal wind in the region of the city of Manaus (Figs. 4C,D,G,H) in relation to the 1st and 2nd, where the zonal wind at the grid point closest in the city of Manaus was −3.97, −4.66, on the 1st and 2nd of August, and − 3.07, −3.24 m s^{-1} on the 3rd and 4th of August, respectively. This scenario favors the intensification of the river breeze as previously observed in other studies (Silva Dias et al., 2004; Lu et al., 2005). It should also be noted that during this period there were no occurrences of cold front that would justify the weakening of these winds (Silva Dias et al., 2004; Camarinha-Neto et al., 2021).

Fig. 5 shows the temperature values obtained experimentally and the simulated values in the experimental sites T0z, T2 and T3. It is possible to notice that the values of both temperatures were quite similar, with synchronized maximums and minimums. Some small variations can be observed, for example: at the T0z site the simulation underestimated the temperature, mainly the minimum temperatures (−0.44 °C). At site T2 the simulation underestimated the maximum temperatures, but overestimated the minimum temperatures (0.33 °C). The temperature behavior at the T3 site was similar to that observed at T2, however slightly overestimating with a mean bias of 0.72 °C. In general, the simulation captured the diurnal temperature variation in the three sites when compared to what was observed, and this is important for the formation of the breeze.

Fig. 6 shows the wind rose with data measured experimentally and simulated at the level closest to the surface of sites (27 m) during the entire integration time and separated in periods of the day (10:00 UTC to 22:00 UTC) and night (23:00 UTC to 09:00 UTC). It is observed that the simulation represented the wind direction well during the day, with the greatest differences occurring during the night, mainly at the T2 site. In general, the simulation tended to slightly overestimate the magnitude of the wind speed at sites T0z, T2 and T3 by 0.76, 1.94 and 1.29 m s^{-1}, respectively.

Fig. 7 shows the experimentally obtained and simulated CO and O_3 concentrations. The simulated CO values were underestimated in relation to those measured at the experimental sites, and due to this, different scales were assumed on the y-axes: the scale of the experimental data is on the left and that of the simulated data on the right of Figs. 7A-C-E. Despite underestimating, it can be seen that the simulation was able to capture the variability of CO at sites T0z, T2 and T3. It is this

Table 3
The mean and standard deviation values of the experimental sites during the month of August, and statistical parameters between experimental and simulated data for Mean Bias (MB), Root Mean Square Error (RMSE) and Pearson correlation coefficient (r).

Variable	Site	Mean	Std	MB	RMSE	r
Temperature (°C)	T0z	26.56	3.1	−0.47	1.82	0.85
	T2	28.52	3.45	−0.33	2.43	0.63
	T3	26.45	3.04	0.73	1.69	0.87
Windspeed (m s^{-1})	T0z	2	0.96	0.76	1.09	0.66
	T2	1.38	1.07	1.94	2.18	0.55
	T3	1.63	1.25	1.29	1.78	0.54
CO (ppbv)	T0z	180	78.06	−37.48	42.24	−0.04
	T2	222	113.48	−65.09	83.27	0.45
	T3	168	37.57	−47.04	57.97	0.36
O_3 (ppbv)	T0z	10.28	10.2	NaN	NaN	NaN
	T2	17.74	15.14	−0.14	10.07	0.50
	T3	16.53	15.02	4.71	11.14	0.71

variability that interests us, since we want to know the role of the river breeze presence on the scalar transport.

For the period investigated in this work, there was no data available for O_3 at the T0z site. It is possible to observe that the simulation was able to show the daily cycle of O_3, that is, the increase during the day and the decrease at night. Furthermore, it is noted that the simulated O_3 values are very close to the experimental values, especially for the daytime period (Figs. 7D-F). Another issue that deserves attention is that the simulation was able to show that the concentrations of CO and O_3 in the T2 and T3 sites were higher than in the T0z site. This occurs since T2 and T3 are located close to the city of Manaus and in the direction of mean flow (Fig. 1) and often pollution plumes from Manaus are transported to T2 and T3, as already shown by several studies (Trebs et al., 2012; Cirino et al., 2018; Camarinha-Neto et al., 2021; D'Oliveira et al., 2022).

Table 3 shows the mean and standard deviation values in the experimental sites during the month of August, and the values of some statistical parameters, such as mean bias (MB), root mean square error (RMSE) and correlation coefficient (r), for obtained from simulated and measured data. Such parameters provide us with information on the effectiveness of the simulation in reproducing the behavior of the experimental data. Note that the r values were >0.5 for all variables and at all sites, except for CO. The RMSE and bias values were also relatively low for all sites and variables, except for CO. As previously mentioned, the simulated CO values were underestimated in relation to the measured data, which is why we obtained high RMSE and MB values. However, the values presented in Table 3 reinforce that the values of the simulated variables are consistent with the observed values.

3.2. River breeze

The following results represent the outputs from the WRF-Chem simulations. Fig. 8 presents the temperature at the 2 m level. The arrows correspond to the difference between the average daily wind speed and the hourly average wind speed at 150 m extracted from the simulation between August 1st and August 4th, 2014. We proceeded in this way so that the breezes are easily identified. The times shown in Fig. 8 correspond to 15:00 UTC. This time was chosen because it was during this period that the river breeze was more intense (Fig. 10). The FOR (Forest) and URB (Urban) ellipses indicate the regions where the most intense breezes and with the greatest temperature contrast were observed.

It was observed that the temperature gradients between the river and the forest region (forest-river) and the river and the urban region (urban-river) intensified over the days, reaching a higher value on the 3rd and 4th of August (Fig. 8). On those days when the temperature gradient was greater, a change in wind direction (from the river towards the continent) is observed. This change marks the entrance of the river breeze in both the Forest and Urban areas. Similar results were found in other breeze circulation studies (Pereira Oliveira and Fitzjarrald, 1993; Silva Dias et al., 2004; Lu et al., 2005;, Saad et al., 2010; Santos et al., 2014; Germano et al., 2017; Corrêa et al., 2021).

Fig. 9 is similar to Fig. 8, and the rectangles RIV (Negro River), FOR (Forest) and URB (Urban) indicate the regions where the most intense breezes and with the greatest temperature contrast were observed. Here we separate the regions where river-forest breezes occur (Figs. 9A-B-C-D) and river-urban breezes (Figs. 9E-F-G-H). Table 4 shows the average temperature at the near surface level for the RIV and FOR area in the Forest region, and RIV and URB in the Urban region represented in Fig. 9, on the 1st, 2nd, 3rd and 4th of August. It is also observed that the

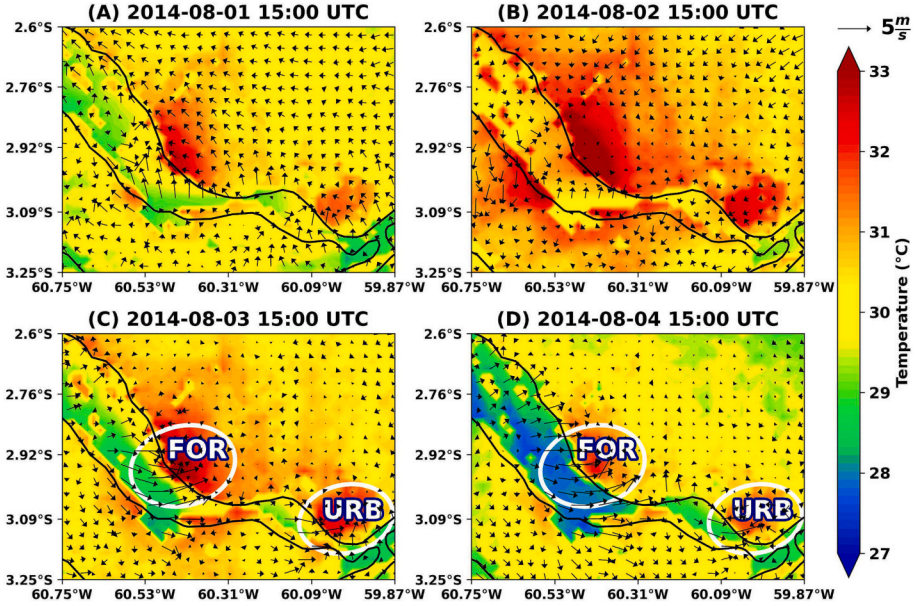

Fig. 8. Temperature (shaded, °C) at 2 m height. The arrows correspond to the difference between the average daily wind speed and the hourly average wind speed at 150 m extracted from the simulation between August 1st and August 4th, 2014. The white ellipses represent the river breeze identified in: (1) Forest (FOR); and (2) Urban (URB).

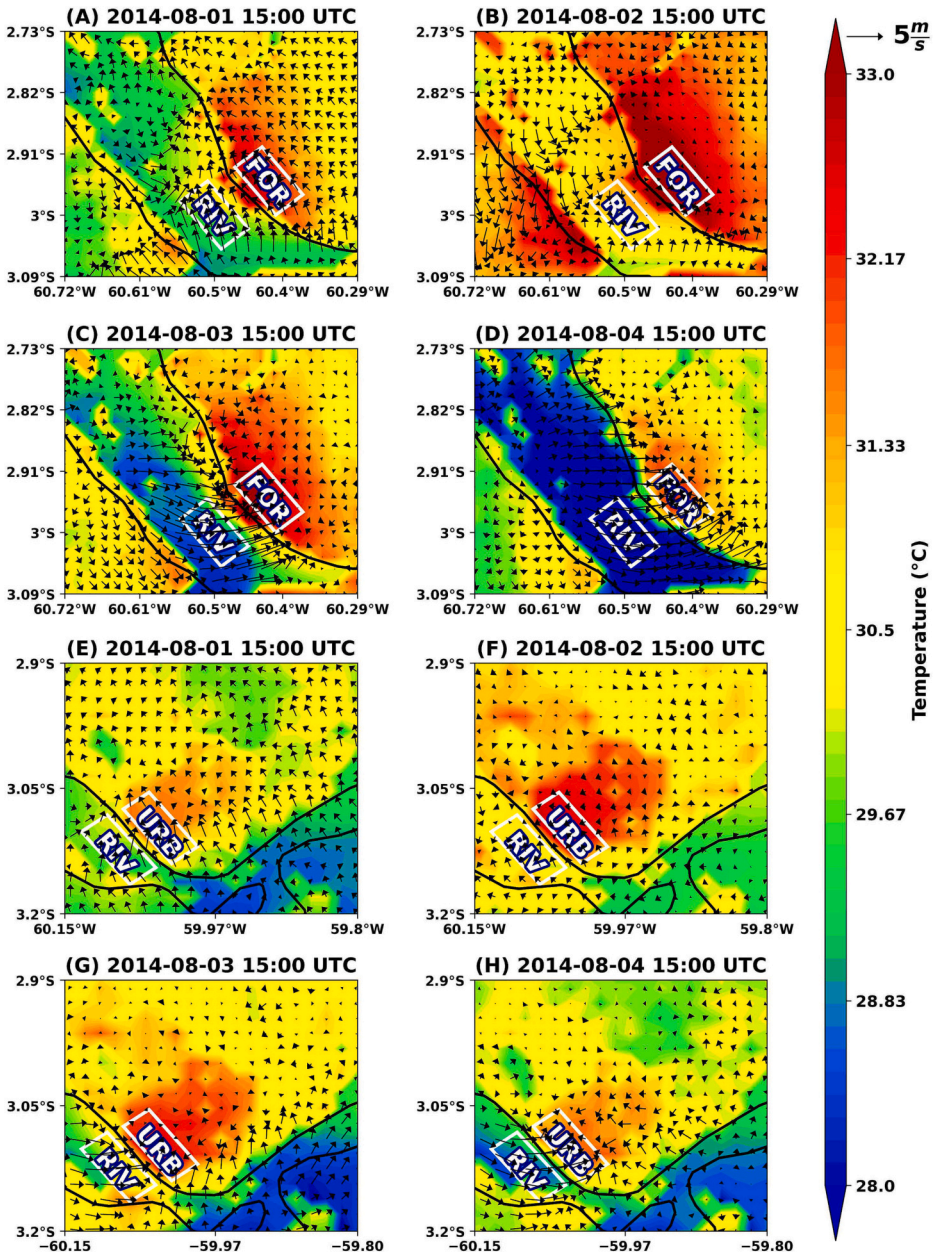

Fig. 9. Zoom in on Fig. 8. Temperature (shaded, °C) at 2 m. The arrows correspond to the difference between the average daily wind speed and the hourly average wind speed at 150 m extracted from the simulation between the entire period. White rectangles indicate the analyzed area in the Negro River (RIV), forest (FOR) and urban (URB).

Table 4
Average simulated temperature in the FOR and URB areas at 2 m in degrees Celcius (°C) during the daytime period (12:00 to 22:00 UTC) on 1st, 2nd, 3rd and 4th of August 2014.

	FOR		URB	
	River	Forest	River	Urban
Day 1	30.06	32.02	30.09	31.54
Day 2	30.98	32.88	30.49	32.16
Day 3	28.85	32.62	30.34	32.24
Day 4	29.1	31.77	29.72	31.65

average temperature over the river decreased over the days, with the lowest average temperature observed on August 4 (reduction of 1.86 °C in the region surrounding the FOR and 0.37 °C in the region surrounding the URB). On the other hand, above the region in FOR and URB the mean temperatures did not show a cooling trend as observed for the river. However, it is noted that the greatest temperature differences between RIV and FOR and RIV and URB occurred on August 3rd, the day on which the breezes had their origins (Figs. 8 and 9).

The temperature difference (ΔT) between FOR and RIV (FOR-RIV) and URB and RIV (URB-RIV) during the first hours of the day throughout the period analyzed for Forest and Urban can be seen in Fig. 10. In the Forest (Fig. 10A) it is evident that the ΔT values were higher on the 3rd and 4th of August. Although these values were similar, on day 4 the river breeze was more intense than on day 3, with the west wind entering the forest area (Fig. 9D). An hypothesis for this occurred is due to the growth of ΔT in the first hours of day 4 (between 10:30 and 14:00 UTC), and it was slightly higher than on the previous day. Furthermore, it is noted that on day 4 the value of ΔT remained approximately constant after the beginning of the breeze period. This is associated with cooling caused by the breeze, an effect that was documented by Zhou et al. (2019) for a

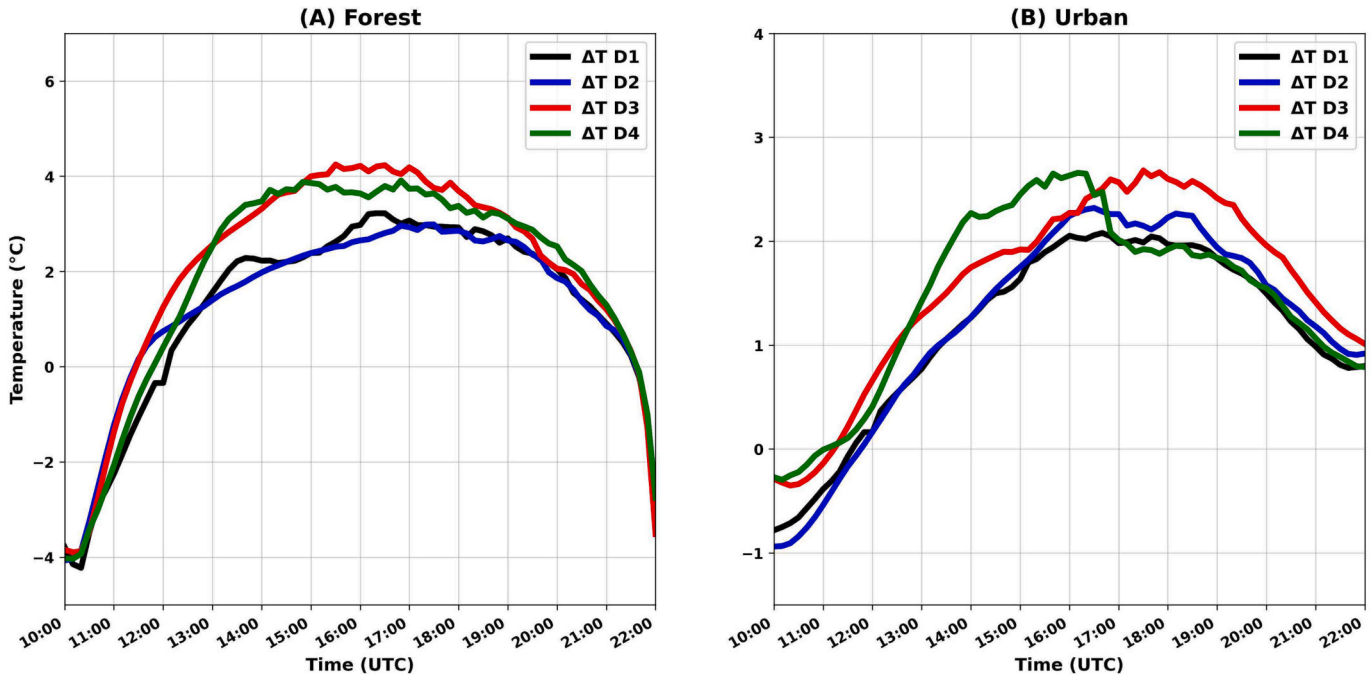

Fig. 10. Simulated difference in temperature at 2 m (ΔT) between FOR and RIV and URB and RIV (°C) for the period from 1st to 4th August 2014 between 10:00 and 22:00 UTC. The solid black line represents the ΔT on day 1 (D1), the solid blue line represents the ΔT on day 2 (D2), the solid red line represents the ΔT on day 3 (D3), and the solid green line represents the ΔT on day 4 (D4). (For interpretation of the references to colour in this figure legend, the reader is referred to the web version of this article.)

coastal city in Australia.

For the Urban area (Fig. 10B) the ΔT values were considerably higher between the times of 13:00 and 16:00 UTC on day 4 and this may explain the greater intensity of the river breeze on that day, compared to day 3. It is noticed that after 16:00 UTC there is a drop in ΔT. This is associated with cooling caused by the breeze, an effect that was observed by Zhou et al. (2019). Another important observation is that on day 4 the ΔT values associated with the river-forest breeze were >1 °C when compared to river-urban breeze values for the same day. This explains why the river breeze is more intense in the Forest region than in the Urban region, and thus, the cooling effect of the forest surface was more evident.

Also in Fig. 10, it can be seen that breezes only occurred when ΔT was >3 °C between forest and river and >2.5 °C between urban and river. That is, the case studies investigated here suggest that there is a temperature threshold for the occurrence of breezes.

The attention has been given to the formation of river breezes, so far, in two regions with different characteristics (FOR and URB) located on the east bank of the Negro River. It was observed that these breezes play an important role in the organization of flow near the surface, as already shown by previous works (Fitzjarrald et al., 2008; Cohen et al., 2014; Lu et al., 2005; Camarinha-Neto et al., 2021) for the Amazonia region. From now on, attention will be given to the role of breeze circulation in the transport of CO and O_3, especially for the urban region of the city of Manaus, where there is a region with significant gas emissions through thermoelectric plants, in addition to the transport of gases from fires in the east of the region.

3.3. Transport of gases

3.3.1. Transport of carbon monoxide

Fig. 11 shows the CO concentration at the level closest to the surface and wind at 150 m on the four days analyzed at 15:00 UTC for Forest (Figs. 11A-B-C-D) and Urban (Figs. 11E-F-G-H) regions. The 1st of August stands out for the high concentrations of CO near the surface. This high concentration is associated with the many fires spots present on August 1 (not shown), several of them located to the east of the regions investigated here, that is, it is believed that CO was transported from the fires to the FOR and URB regions. On August 4th, fires were located predominantly to the south, and therefore had little influence on CO concentrations in the regions investigated here.

In Forest, on day 3, the breeze was weaker than on day 4 (Fig. 10). This becomes evident when analyzing CO transport (Fig. 11C-D). Note that the breeze keeps the air with higher concentrations of CO on the east bank of the Negro River (Fig. 11D). In Urban, the river breeze on day 3 (Fig. 11G) is barely perceptible. The influence of the river breeze is more evident on day 4 (Fig. 11H), where the westerly winds from the breeze meet the east winds on the west bank of the city of Manaus. In this region, it is possible to notice that the breeze also maintains the air with higher concentrations of CO in the western portion of the city of Manaus.

The difference between the two regions can be observed both in the intensity of the river breeze and in the concentrations of CO. Except for August 1st, it is observed that CO concentrations are lower in Forest, however, it is noted that there is a CO plume being transported from the east to the region. While in the Urban region, it is possible to see that the emission of the city of Manaus is continuous, which is associated with thermoelectric plants and cars in the region, and therefore in this region there are greater amounts of CO even if there are no large fire spots in the east of the city.

To further explore the effects of river breezes on CO transport, vertical cross sections were made at latitudes of 2.964°S and 3.1079°S for Forest and Urban, respectively, from the closest surface level to 1200 m on August 4th, the day in which that the breeze was more intense in both regions (Fig. 12).

A first observation to be mentioned is that the breeze (west winds) is relatively shallow, not exceeding 400 m in height. In Forest, four different hours were analyzed: 15:00, 16:00, 17:00 and 18:00 UTC (Figs. 12A-B-C-D). A CO plume can be seen between 1000 and 1200 m being transported from the east, while the breeze is seen entering the forest region (the river bank is represented by the dashed line) (Fig. 12A). Over time, the CO plume is transported from east to west, however, the region where the river breeze and the prevailing winds

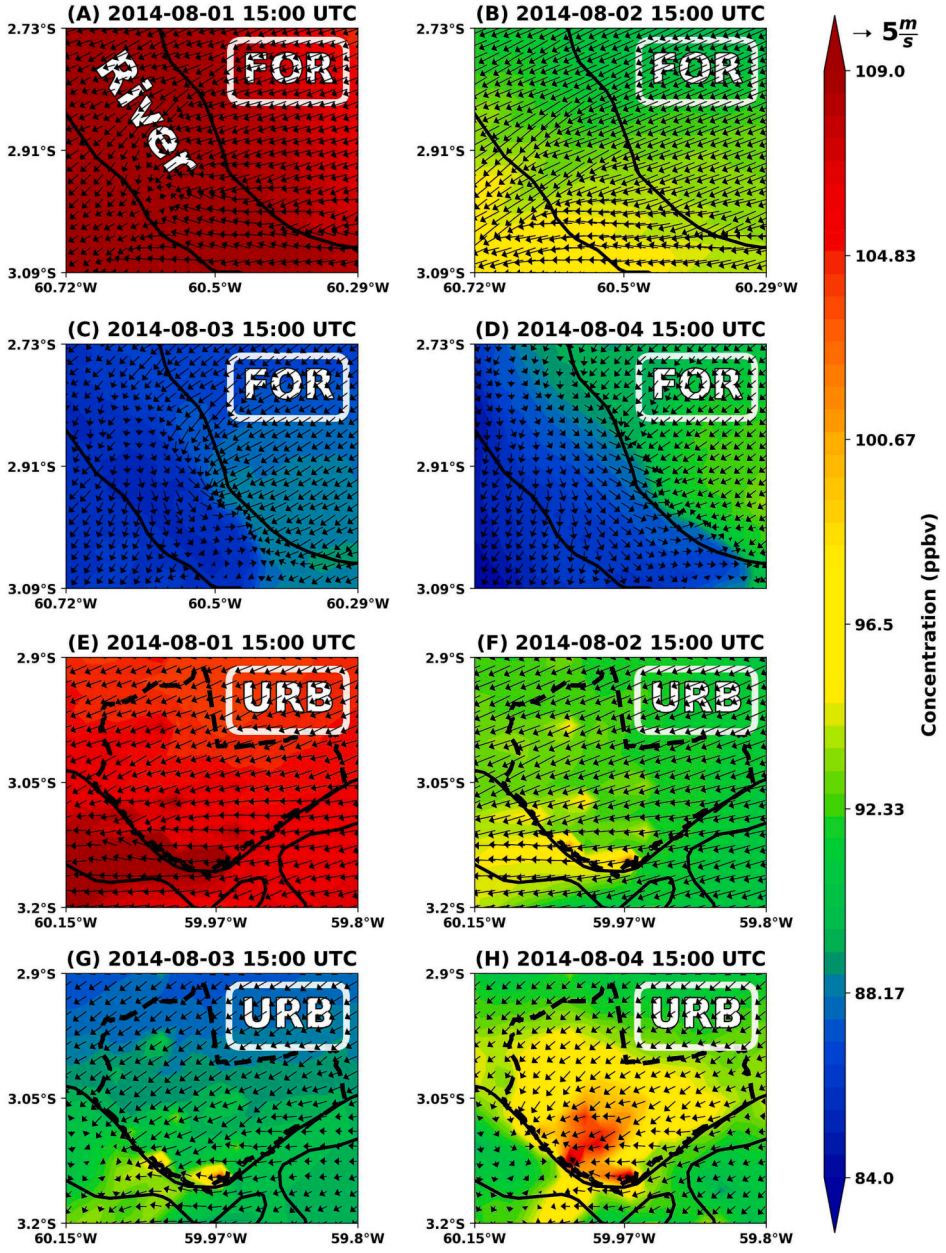

Fig. 11. CO concentration (shaded, ppbv) near surface and wind (arrow, m s^{-1}) over 150 m between August 1st and 4th, 2014 at 15:00 UTC in: (A), (B), (C) and (D) for Forest; (E), (F), (G) and (H) for Urban. The area of the Negro River in Forest is indicated in (A) as River, and the urban area of the city of Manaus is represented by the black dashed line in (E), (F), (G) and (H).

converge shows an area with different concentrations of CO, which can be seen as a "CO front region". This region of confluence of the winds causes the CO coming from the east to be transported upwards, and thus the flow to the east continues, but above the breeze circulation. However, this circulation causes this air mass with high concentrations of CO to descend in a region of the river, and distributed in the region of the Negro River. This result corroborates the results found by Zhao et al. (2021), where the authors observed a region of recirculation of pollutants near the city of Manaus, in a forest region.

In Urban, it is noted that there is a similar behavior. Again, four different hours were analyzed: 14:00, 15:00, 16:00 and 17:00 UTC (Figs. 12E-F-G-H), being different from the times of Forest due to the river breeze being weaker, and therefore, a shorter duration. The Manaus city region is represented between the two black dashed lines. It is observed that the breeze did not enter the urban area. It is noteworthy that the region with the highest concentrations of CO can be observed in the eastern region of the city at 14:00 UTC (industrial region of the city). At 15:00 and 16:00 UTC, the breeze traps CO in the west region of the city (Fig. 12G).

3.3.2. *Transport of ozone*

The city of Manaus is a major source of O_3 in the central Amazonia region (Kuhn et al., 2010) due to its intense vehicular and industrial activity, which causes a great contrast with the surrounding forest area. With that in mind, we analyze how the breeze can influence O_3 transport in the Forest and Urban regions.

Fig. 13 shows the O_3 concentration at the level closest to the surface and the wind at 150 m on the four days analyzed at 15:00 UTC for Forest (Figs. 13A-B-C-D) and Urban (Figs. 13E-F-G-H). Opposite to what was observed with CO, the environment on day 1 was not a day with high O_3 concentrations in either region. In Forest, the days that stand out are the days when there is a river breeze on the east bank of the Negro river

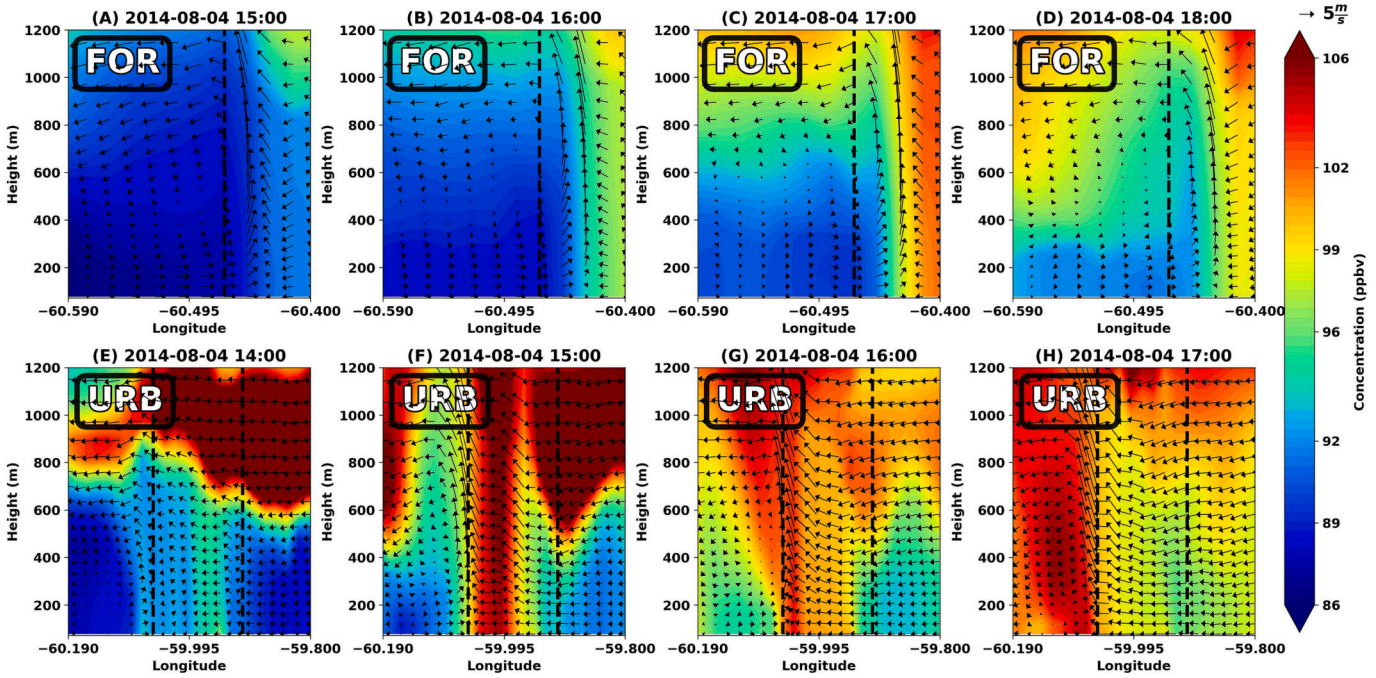

Fig. 12. Vertical cross section at latitude 2.964°S for Forest and 3.1079°S for Urban up to 1200 m of CO concentration (shaded, ppbv) zonal and vertical wind multiplied by 10 (u;w*10) (arrows, m s^{-1}) on August 4th, 2014 for FOR in: (A) 15:00 UTC; (B) 16:00 UTC; (C) 17:00 UTC; (D) 18:00 UTC, and for URB in: (E) 14:00 UTC; (F) 15:00 UTC; (G) 16:00 UTC; e (H) 17:00 UTC. The dashed line in (A), (B), (C) and (D) represents the bank of the Negro river, and in (E), (F), (G) and (H), it represents the limits of the urban region from Manaus.

(Figs. 13C-D). As observed with CO, the breeze also traps air with higher concentrations of O_3 in the wind confluence region. Another point to note is that the 4th of August was the day when there are the lowest concentrations of O_3 in this region.

In Urban region there is intense urban activity, and therefore it is expected that O_3 concentrations are higher when compared to Forest. Figs. 13E-F-G-H show that, contrary to what was observed in Fig. 11, where there was a source of CO in the city of Manaus, it now shows that these points act as sinks for O_3, however, a few kilometers to the east of these sinks, it is possible to see a region with higher concentrations. These lower concentrations of O_3 can be explained by the presence of thermoelectric plants that emit NO_x (NO and NO_2), which acts as an O_3 sink in some environments (Ryerson et al., 2001). In addition, Arin and Warneck (1972) show that there is also a possibility of interaction between O_3 and CO to form CO_2 and O_2, that is, where there are large sources of CO, these can act as an O_3 sink. Therefore, the highest concentrations of O_3 will be found west of its source of emission (west of the city of Manaus) due to the transport of easterly winds. However, although O_3 has its highest concentrations in the Negro River region, on August 4th it is possible to notice that there is a region with high concentrations of O_3 in the western portion of the city.

Fig. 14 shows the vertical section of the O_3 concentration in Forest (Figs. 14A-B-C-D) and in Urban (Figs. 14E-F-G-H) through the same analysis performed for CO in Fig. 12. In Forest, the O_3 plume can be seen being transported from the east until it finds the confluence region of the winds and is observed as an "O_3 frontal region" (Figs. 14B-C). In the same way as observed with CO, it is seen that the O_3 plume is transported over the breeze circulation, as well as part of this air mass with slightly higher O_3 concentrations, descends and is distributed in the Negro River region.

In Urban an O_3 plume is observed above 600 m at 14:00 UTC throughout the analyzed area (Fig. 14E). As the river breeze intensifies, it is noted that in the region where the confluence of the winds is observed, an air mass with lower concentrations of O_3 is transported to levels above 1000 m, as well as there is also a recirculation through the river breeze circulation at levels close to the ground (Fig. 14F). It is noteworthy that during the entire period analyzed in Urban, no large concentrations of O_3 were observed in the area between longitudes 59.975°W and 59.8°W, which represent the eastern regions of the city of Manaus and the Negro River.

4. Conclusions

Through numerical simulations with the WRF-Chem model, the river breeze circulations of the Negro River were investigated, in the region of the city of Manaus (Urban) and a forest region northeast of the city (Forest), both localized in the central Amazonia region, during the period from 1st to 4th of August 2014. The formation of the river breeze and its influence on the transport of gases such as O_3 and CO in urban and forest areas were analyzed. The results showed that the WRF-Chem model was able to satisfactorily represent the meteorological variables and the O_3 concentrations. The CO concentrations were underestimated by the model, however the CO variability was well represented by the simulations.

The Negro River is an important river in the central Amazonia, which also borders the city of Manaus. Its geographical location close to the city makes the river breeze in the west region responsible for winds in the opposite direction to the east winds, which are predominant in the region. The mechanism that leads to the formation of the breeze was explored in two different areas: a region with contrast between river and forest west of Manaus, and the region of contrast with the river and the urban area of Manaus.

The results show that the formation of the breeze, in addition to the favorable large-scale condition with the weakening of the easterly winds, was dependent on the temperature variation of the Negro River. These results corroborate other studies that show the same behavior in other places in the Amazonia region. It is also concluded that the temperature difference between the river and the ground is important during the first hours of the day.

During the analyzed period, the formation of a river breeze was observed in both regions in two days (August 3rd and 4th). The change in the direction of the winds caused by the river breeze has implications

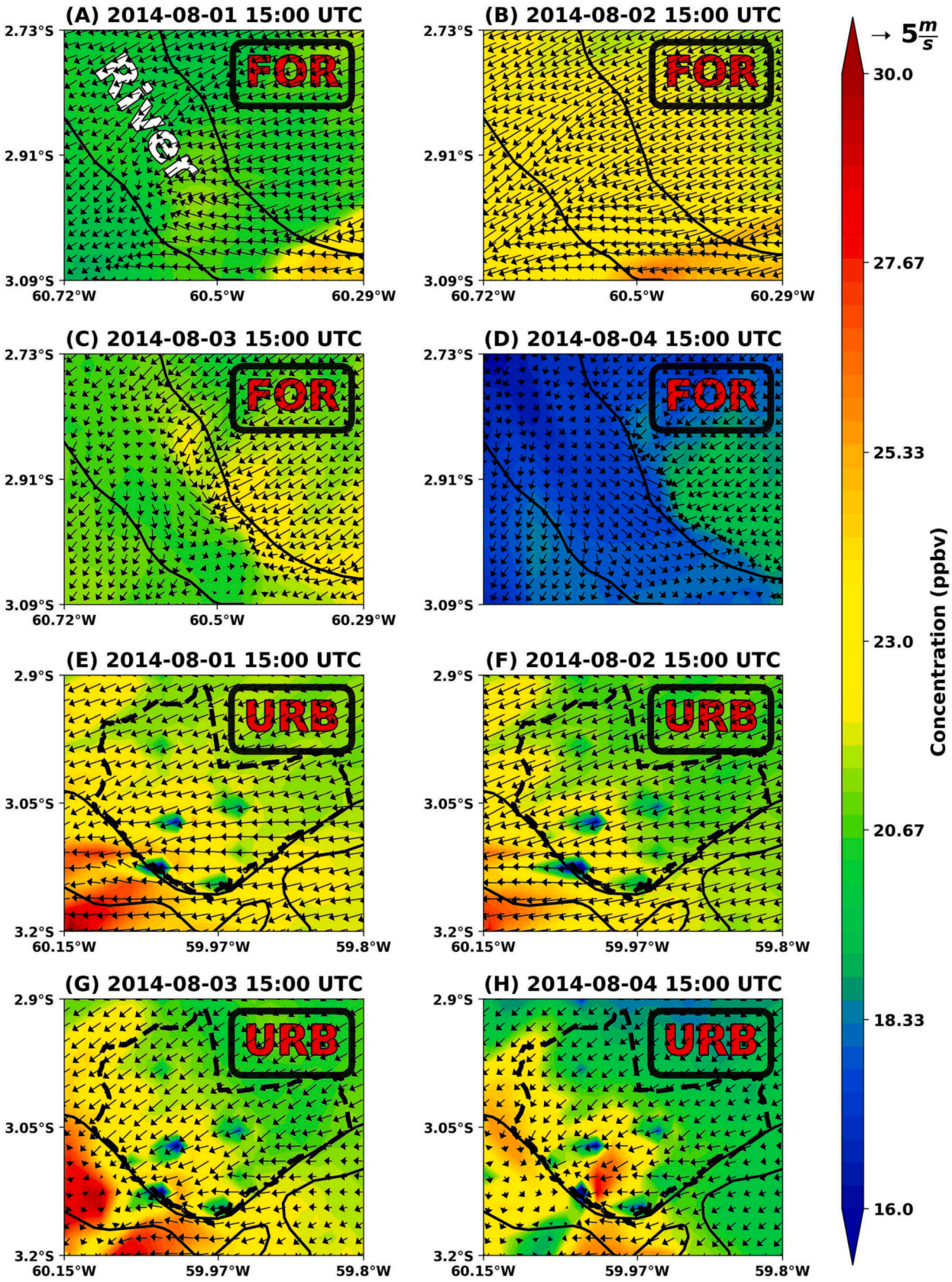

Fig. 13. O_3 concentration (shaded, ppbv) near the surface and wind at 150 m (arrows, m s^{-1}) in Forest: (A) 15:00 UTC on the August, 1st; (b) 15:00 UTC on the August, 2nd; 15:00 UTC on the August, 3rd; and (D) 15:00 UTC on August, 4th of 2014. The area of the Negro River in Forest is indicated in (A) as River, and the urban area of the city of Manaus is represented by the black dashed line in (E), (F), (G) and (H).

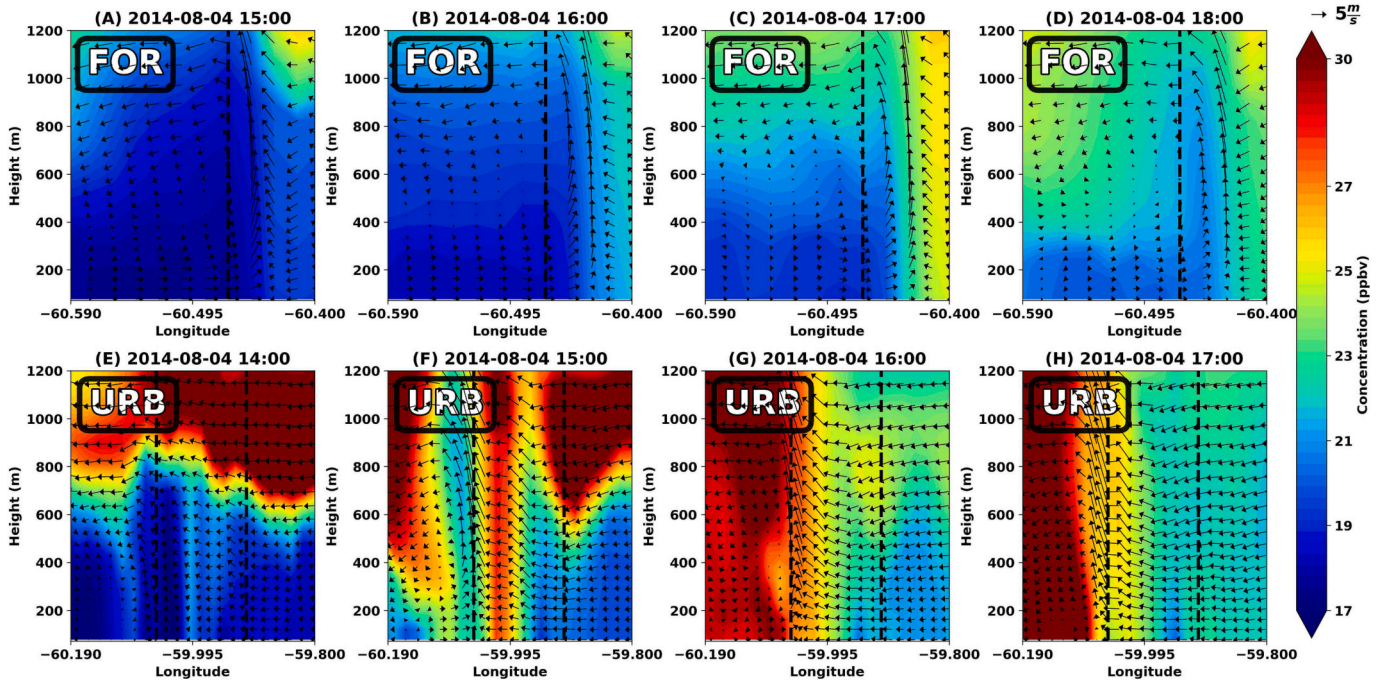

Fig. 14. Vertical cross section at latitude 2.964°S for Forest and 3.1079°S for Urban up to 1200 m of O_3 concentration (shaded, ppbv), zonal and vertical wind multiplied by 10 (u;w*10) (arrows, m s^{-1}) on August, 4th of 2014 for FOR in: (A) 15:00 UTC; (B) 16:00 UTC; (C) 17:00 UTC; (D) 18:00 UTC, and to URB in: (E) 14:00 UTC; (F) 15:00 UTC; (G) 16:00 UTC; and (H) 17:00 UTC. The dashed line in (A), (B), (C) and (D) represents the bank of the Negro River, and in (E), (F), (G) and (H), it represents the limits of the urban region from Manaus.

for the concentrations of CO and O_3 in the confluence region of the winds, delaying advection to the west during the period when the breeze is active.

In the Forest region, the breeze was more intense, and because of that, it kept the CO and O_3 on the east bank of the Negro River at levels closer to the surface, as well as the circulation caused the gases to be transported to higher levels. Since O_3 is associated with a reduction in gross primary production in forests (Pacifico et al., 2015; Yue and Unger, 2018), scenarios in which there is an increase in concentrations of this gas at levels close to the surface, together with trapping in regions where the river breeze occurs, can represent a growing threat to the productivity of the ecosystem. In addition high O_3 concentrations are a risk to the people who live on the banks of the rivers. In the Urban region, it was seen that the breeze was less intense and had a shorter duration, however, it was still able to maintain higher concentrations of CO and O_3 in the western region of the city of Manaus.

These results show a concern about future scenarios of climate change and increased deforestation, fires and urbanization in the Amazonia. With greater emissions of pollutants, the risk caused to those living in the affected regions also increases. Another point to note is that the gases emitted into the city of Manaus end up being trapped in the western region, which is predominantly residential.

CRediT authorship contribution statement

Flávio A.F. D'Oliveira: Conceptualization, Methodology, Writing – original draft, Writing – review & editing, Formal analysis. **Cleo Q. Dias-Júnior:** Conceptualization, Methodology, Writing – review & editing, Formal analysis. **Julia C.P. Cohen:** Conceptualization, Methodology, Writing – review & editing, Formal analysis. **Dominick V. Spracklen:** Methodology, Writing – review & editing. **Edson P. Marques-Filho:** Writing – review & editing. **Paulo Artaxo:** Data curation.

Declaration of Competing Interest

The authors declare that they have no known competing financial interests or personal relationships that could have appeared to influence the work reported in this paper.

Data availability

Data will be made available on request.

Acknowledgements

We acknowledge support from the Atmospheric Radiation Measurement (ARM) Climate Research Facility, a user facility of the United States Department of Energy (DOE) for the experimental T3 site data. We acknowledge the LBA Micrometeorology Lab, especially, Antônio Manzi, Alessandro C. de Araujo, Marta Sá, Leila Leal, Paulo Teixeira and Leonardo R. de Oliveira for all the support (maintenance and processing of T0z data). Flávio A. F. D'Oliveira acknowledges CAPES (Coordenação de Aperfeiçoamento de Pessoal de Nível Superior) grant n. 88882.445444/2019-01 for the PhD scholarship and the support of a Royal Society Newton Advanced Fellowship (NAF\R1\180405). This work was undertaken on ARC3, part of the High Performance Computing facilities at the University of Leeds, UK. Cleo Q. Dias-Junior acknowledges the support from CNPq (Processes 440170/2022-2, 406884/2022-6, 307530/2022-1). P. Artaxo acknowledges the FAPESP (Fundação de Amparo à Pesquisa do Estado de São Paulo) grant 2017/17047-0.

References

Ainsworth, E.A., Yendrek, C.R., Sitch, S., Collins, W.J., Emberson, L.D., 2012. The effects of tropospheric ozone on net primary productivity and implications for climate change. Annu. Rev. Plant Biol. 63, 637–661. https://doi.org/10.1146/annurev-arplant-042110-103829.

Andreae, M., Artaxo, P., Beck, V., Bela, M., Freitas, S., Gerbig, C., Longo, K., Munger, J., Wiedemann, K., Wofsy, S., 2012. Carbon monoxide and related trace gases and

aerosols over the amazon basin during the wet and dry seasons. Atmos. Chem. Phys. 12, 6041–6065. https://doi.org/10.5194/acp-12-6041-2012.
Arin, L.M., Warneck, P., 1972. Reaction of ozone with carbon monoxide. J. Phys. Chem. 76, 1514–1516. https://doi.org/10.1021/j100655a002.
Arritt, R.W., 1993. Effects of the large-scale flow on characteristic features of the sea breeze. J. Appl. Meteorol. Climatol. 32, 116–125. https://doi.org/10.1175/1520-0450(1993)032<0116:EOTLSF>2.0.CO;2.
Avnery, S., Mauzerall, D.L., Liu, J., Horowitz, L.W., 2011. Global crop yield reductions due to surface ozone exposure: 1. Year 2000 crop production losses and economic damage. Atmos. Environ. 45, 2284–2296. https://doi.org/10.1016/j.atmosenv.2010.11.045.
Barlow, J., Berenguer, E., Carmenta, R., França, F., 2020. Clarifying amazonia's burning crisis. Glob. Chang. Biol. 26, 319–321. https://doi.org/10.1111/gcb.14872.
Bechtold, P., Pinty, J.P., Mascart, F., 1991. A numerical investigation of the influence of large-scale winds on sea-breeze-and inland-breeze-type circulations. J. Appl. Meteorol. Climatol. 30, 1268–1279. https://doi.org/10.1175/1520-0450(1991)030<1268:ANIOTI>2.0.CO;2.
Bernardini, F., Attademo, L., Trezzi, R., Gobbicchi, C., Balducci, P., Del Bello, V., Menculini, G., Pauselli, L., Piselli, M., Sciarma, T., et al., 2020. Air pollutants and daily number of admissions to psychiatric emergency services: evidence for detrimental mental health effects of ozone. Epidemiol. Psychiatr. Sci. 29, e66 https://doi.org/10.1017/S2045796019000623.
Betts, A.K., Gatti, L.V., Cordova, A.M., Silva Dias, M.A., Fuentes, J.D., 2002. Transport of ozone to the surface by convective downdrafts at night. J. Geophys. Res.-Atmos. 107 https://doi.org/10.1029/2000JD000158. LBA–13.
Bleecker, M.L., 2015. Carbon monoxide intoxication. Handb. Clin. Neurol. 131, 191–203. https://doi.org/10.1016/B978-0-444-62627-1.00024-X.
Block, M.L., Elder, A., Auten, R.L., Bilbo, S.D., Chen, H., Chen, J.C., Cory-Slechta, D.A., Costa, D., Diaz-Sanchez, D., Dorman, D.C., et al., 2012. The outdoor air pollution and brain health workshop. Neurotoxicology 33, 972–984. https://doi.org/10.1016/j.neuro.2012.08.014.
Borne, K., Chen, D., Nunez, M., 1998. A method for finding sea breeze days under stable synoptic conditions and its application to the swedish west coast. Int. J. Climatol. 18, 901–914. https://doi.org/10.1002/(SICI)1097-0088(19980630)18:8<901::AID-JOC295>3.0.CO;2-F.
Bourgeois, I., Peischl, J., Neuman, J.A., Brown, S.S., Thompson, C.R., Aikin, K.C., Allen, H.M., Angot, H., Apel, E.C., Baublitz, C.B., et al., 2021. Large contribution of biomass burning emissions to ozone throughout the global remote troposphere. Proc. Natl. Acad. Sci. 118, e2109628118 https://doi.org/10.1073/pnas.2109628118.
Boyouk, N., Léon, J.F., Delbarre, H., Augustin, P., Fourmentin, M., 2011. Impact of sea breeze on vertical structure of aerosol optical properties in dunkerque, France. Atmos. Res. 101, 902–910. https://doi.org/10.1016/j.atmosres.2011.05.016.
Bush, M.L., Asplund, P.T., Miles, K.A., Ben-Jebria, A., Ultman, J.S., 1996. Longitudinal distribution of o3 absorption in the lung: gender differences and intersubject variability. J. Appl. Physiol. 81, 1651–1657. https://doi.org/10.1152/jappl.1996.81.4.1651.
Camarinha-Neto, G.F., Cohen, J.C., Dias-Júnior, C.Q., Sörgel, M., Cattanio, J.H., Araújo, A., Wolff, S., Kuhn, P.A., Souza, R.A., Rizzo, L.V., et al., 2021. The friagem event in the central amazon and its influence on micrometeorological variables and atmospheric chemistry. Atmos. Chem. Phys. 21, 339–356. https://doi.org/10.5194/acp-21-339-2021.
Cano-Crespo, A., Traxl, D., Thonicke, K., 2021. Spatio-temporal patterns of extreme fires in amazonian forests. Eur. Phys. J. Spec. Top. 230, 3033–3044. https://doi.org/10.1140/epjs/s11734-021-00164-3.
Chen, K., Breitner, S., Wolf, K., Stafoggia, M., Sera, F., Vicedo-Cabrera, A.M., Guo, Y., Tong, S., Lavigne, E., Matus, P., et al., 2021. Ambient carbon monoxide and daily mortality: a global time-series study in 337 cities. Lancet Planet. Health 5, e191–e199. https://doi.org/10.1016/S2542-5196(21)00026-7.
Cheng, H., Sinha, A., Cruz, F.W., Wang, X., Edwards, R.L., d'Horta, F.M., Ribas, C.C., Vuille, M., Stott, L.D., Auler, A.S., 2013. Climate change patterns in Amazonia and biodiversity. Nat. Commun. 4, 1411. https://doi.org/10.1038/ncomms2415.
Cirino, G., Brito, J., Barbosa, H.M., Rizzo, L.V., Tunved, P., de Sá, S.S., Jimenez, J.L., Palm, B.B., Carbone, S., Lavric, J.V., et al., 2018. Observations of Manaus urban plume evolution and interaction with biogenic emissions in goamazon 2014/5. Atmos. Environ. 191, 513–524. https://doi.org/10.1016/j.atmosenv.2018.08.031.
Cohen, J.C.P., Fitzjarrald, D.R., D'Oliveira, F.A.F., Saraiva, I., Barbosa, I.R.D.S., Gandu, A.W., Kuhn, P.A., 2014. Radar-observed spatial and temporal rainfall variability near the tapajós-amazon confluence. Rev. Brasil. Meteorol. 29, 23–30. https://doi.org/10.1590/0102-778620130058.
Corrêa, P.B., Dias-Júnior, C.Q., Cava, D., Sörgel, M., Bota, S., Acevedo, O., Oliveira, P.E., Manzi, A.O., Machado, L.A.T., dos Santos Martins, H., et al., 2021. A case study of a gravity wave induced by amazon forest orography and low level jet generation. Agric. For. Meteorol. 307, 108457. https://doi.org/10.1016/j.agrformet.2021.108457.
Crutzen, P.J., Andreae, M.O., 1990. Biomass burning in the tropics: Impact on atmospheric chemistry and biogeochemical cycles. Science 250, 1669–1678. https://doi.org/10.1126/science.250.4988.1669.
Dentener, F., Kinne, S., Bond, T., Boucher, O., Cofala, J., Generoso, S., Ginoux, P., Gong, S., Hoelzemann, J., Ito, A., et al., 2006. Emissions of primary aerosol and precursor gases in the years 2000 and 1750 prescribed data-sets for aerocom. Atmos. Chem. Phys. 6, 4321–4344. https://doi.org/10.5194/acp-6-4321-2006.
DETRAN, 2022. Frota de veículos no amazonas cresceu 4% em 2021. <https://www.detran.am.gov.br/frota-de-veiculos-no-amazonas-cresceu-4-em-2021/>. Accessed 06.04.22.
Dias-Junior, C.Q., Dias, N.L., Fuentes, J.D., Chamecki, M., 2017. Convective storms and non-classical low-level jets during high ozone level episodes in the amazon region: an arm/goamazon case study. Atmos. Environ. 155, 199–209. https://doi.org/10.1016/j.atmosenv.2017.02.006.
D'Oliveira, F.A.F., Cohen, J.C.P., Spracklen, D.V., Medeiros, A.S.S., Cirino, G.G., Artaxo, P., Dias-Júnior, C.Q., 2022. Simulation of the effects of biomass burning in a mesoscale convective system in the central amazon. Atmos. Res. 278, 106345. https://doi.org/10.1016/j.atmosres.2022.106345.
ELETROBRÁS, 2014. Operation. <https://eletrobras.com/en/Paginas/Operacao.aspx>. Accessed 11.12.20.
Faulstich, S.D., Schissler, A.G., Strickland, M.J., Holmes, H.A., 2022. Statistical comparison and assessment of four fire emissions inventories for 2013 and a large wildfire in the western United States. Fire 5, 27. https://doi.org/10.3390/fire5010027.
Fitzjarrald, D.R., Sakai, R.K., Moraes, O.L., Cosme de Oliveira, R., Acevedo, O.C., Czikowsky, M.J., Beldini, T., 2008. Spatial and temporal rainfall variability near the amazon-tapajós confluence. J. Geophys. Res. Biogeosci. 113 https://doi.org/10.1029/2007JG000596.
Furberg, M., Steyn, D., Baldi, M., 2002. The climatology of sea breezes on Sardinia. Int. J. Climatol. 22, 917–932. https://doi.org/10.1002/joc.780.
Germano, M.F., Vitorino, M.I., Cohen, J.C.P., Costa, G.B., Souto, J.I.D.O., Rebelo, M.T.C., de Sousa, A.M.L., 2017. Analysis of the breeze circulations in eastern amazon: an observational study. Atmos. Sci. Lett. 18, 67–75. https://doi.org/10.1002/asl.726.
Ghude, S.D., Kumar, R., Jena, C., Debnath, S., Kulkarni, R.G., Alessandrini, S., Biswas, M., Kulkrani, S., Pithani, P., Kelkar, S., et al., 2020. Evaluation of pm2.5 forecast using chemical data assimilation in the wrf-chem model: a novel initiative under the ministry of earth sciences air quality early warning system for Delhi, India. Curr. Sci. 118, 1803–1815. Doi:10.18520/cs/v118/i11/1803-1815.
Giglio, L., 2007. Characterization of the tropical diurnal fire cycle using virs and modis observations. Remote Sens. Environ. 108, 407–421. https://doi.org/10.1016/j.rse.2006.11.018.
Giglio, L., Descloitres, J., Justice, C.O., Kaufman, Y.J., 2003. An enhanced contextual fire detection algorithm for MODIS. Remote Sens. Environ. 87, 273–282. https://doi.org/10.1016/s0034-4257(03)00184-6.
Gonzalez-Alonso, L., Val Martin, M., Kahn, R.A., 2019. Biomass-burning smoke heights over the amazon observed from space. Atmos. Chem. Phys. 19, 1685–1702. https://doi.org/10.5194/acp-19-1685-2019.
Grell, G.A., Peckham, S.E., Schmitz, R., McKeen, S.A., Frost, G., Skamarock, W.C., Eder, B., 2005. Fully coupled "online" chemistry within the WRF model. Atmos. Environ. 39, 6957–6975. https://doi.org/10.1016/j.atmosenv.2005.04.027.
Grulke, N., Heath, R., 2020. Ozone effects on plants in natural ecosystems. Plant Biol. 22, 12–37. https://doi.org/10.1111/plb.12971.
Guenther, A., Karl, T., Harley, P., Wiedinmyer, C., Palmer, P.I., Geron, C., 2006. Estimates of global terrestrial isoprene emissions using MEGAN (Model of Emissions of Gases and Aerosols from Nature). Atmos. Chem. Phys. 6, 3181–3210. https://doi.org/10.5194/acp-6-3181-2006.
Hersbach, H., Bell, B., Berrisford, P., Hirahara, S., Horányi, A., Muñoz-Sabater, J., Nicolas, J., Peubey, C., Radu, R., Schepers, D., Simmons, A., Soci, C., Abdalla, S., Abellan, X., Balsamo, G., Bechtold, P., Biavati, G., Bidlot, J., Bonavita, M., Chiara, G., Dahlgren, P., Dee, D., Diamantakis, M., Dragani, R., Flemming, J., Forbes, R., Fuentes, M., Geer, A., Haimberger, L., Healy, S., Hogan, R.J., Hólm, E., Janisková, M., Keeley, S., Laloyaux, P., Lopez, P., Lupu, C., Radnoti, G., Rosnay, P., Rozum, I., Vamborg, F., Villaume, S., Thépaut, J.N., 2020. The ERA5 global reanalysis. Q.J.R. Meteorol. Soc. 146, 1999–2049. https://doi.org/10.1002/qj.3803.
Hollaway, M.J., Arnold, S., Challinor, A.J., Emberson, L., 2012. Intercontinental trans-boundary contributions to ozone-induced crop yield losses in the northern hemisphere. Biogeosciences 9, 271–292. https://doi.org/10.5194/bg-9-271-2012.
Hrebtov, M., Hanjalić, K., 2019. River-induced anomalies in seasonal variation of traffic-emitted co distribution over the city of Krasnoyarsk. Atmosphere 10, 407. https://doi.org/10.3390/atmos10070407.
Ibarra-Espinosa, S., Ynoue, R., OSullivan, S., Pebesma, E., de Fátima Andrade, M., Osses, M., 2018. VEIN v0.2.2: an r package for bottom–up vehicular emissions inventories. Geosci. Model Dev. 11, 2209–2229. https://doi.org/10.5194/gmd-11-2209-2018.
IBGE, 2022. Manaus. <https://cidades.ibge.gov.br/brasil/am/manaus/panorama/>. Accessed 06.04.22.
Janssens-Maenhout, G., Crippa, M., Guizzardi, D., Muntean, M., Schaaf, E., Dentener, F., Bergamaschi, P., Pagliari, V., Olivier, J.G.J., Peters, J.A.H.W., van Aardenne, J.A., Monni, S., Doering, U., Petrescu, A.M.R., Solazzo, E., Oreggioni, G.D., 2019. EDGAR v4.3.2 global atlas of the three major greenhouse gas emissions for the period 1970–2012. Earth Syst. Sci. Data 11, 959–1002. https://doi.org/10.5194/essd-11-959-2019.
Jiang, L., Liu, S., Liu, C., Feng, Y., 2021. How do urban spatial patterns influence the river cooling effect? A case study of the huangpu riverfront in shanghai, China. Sustain. Cities Soc. 69, 102835. https://doi.org/10.1016/j.scs.2021.102835.
Koman, P.D., Mancuso, P., 2017. Ozone exposure, cardiopulmonary health, and obesity: a substantive review. Chem. Res. Toxicol. 30, 1384–1395. https://doi.org/10.1021/acs.chemrestox.7b00077.
Kuhn, U., Ganzeveld, L., Thielmann, A., Dindorf, T., Schebeske, G., Welling, M., Sciare, J., Roberts, G., Meixner, F., Kesselmeier, J., et al., 2010. Impact of Manaus city on the amazon green ocean atmosphere: ozone production, precursor sensitivity and aerosol load. Atmos. Chem. Phys. 10, 9251–9282. https://doi.org/10.5194/acp-10-9251-2010.
Lamarque, J.F., Emmons, L.K., Hess, P.G., Kinnison, D.E., Tilmes, S., Vitt, F., Heald, C.L., Holland, E.A., Lauritzen, P.H., Neu, J., Orlando, J.J., Rasch, P.J., Tyndall, G.K., 2012. CAM-chem: description and evaluation of interactive atmospheric chemistry in the community earth system model. Geosci. Model Dev. 5, 369–411. https://doi.org/10.5194/gmd-5-369-2012.

Lapola, D.M., Oyama, M.D., Nobre, C.A., Sampaio, G., 2008. A new world natural vegetation map for global change studies. An. Acad. Bras. Cienc. 80, 397–408. https://doi.org/10.1590/S0001-37652008000200017.
Levy, R.J., 2015. Carbon monoxide pollution and neurodevelopment: a public health concern. Neurotoxicol. Teratol. 49, 31–40. https://doi.org/10.1016/j.ntt.2015.03.001.
Li, W., Wang, Y., Bernier, C., Estes, M., 2020. Identification of sea breeze recirculation and its effects on ozone in houston, tx, during discover-aq 2013. J. Geophys. Res.-Atmos. 125, e2020JD033165 https://doi.org/10.1029/2020JD033165.
Lu, L., Denning, A.S., da Silva-Dias, M.A., da Silva-Dias, P., Longo, M., Freitas, S.R., Saatchi, S., 2005. Mesoscale circulations and atmospheric co2 variations in the tapajós region, pará, Brazil. J. Geophys. Res. Atmos. 110 https://doi.org/10.1029/2004JD005757.
Malhi, Y., Roberts, J.T., Betts, R.A., Killeen, T.J., Li, W., Nobre, C.A., 2008. Climate change, deforestation, and the fate of the amazon. Science 319, 169–172. https://doi.org/10.1126/science.1146961.
Marenco, F., Johnson, B., Langridge, J.M., Mulcahy, J., Benedetti, A., Remy, S., Jones, L., Szpek, K., Haywood, J., Longo, K., et al., 2016. On the vertical distribution of smoke in the amazonian atmosphere during the dry season. Atmos. Chem. Phys. 16, 2155–2174. https://doi.org/10.5194/acp-16-2155-2016.
Marengo, J., 2005. The characteristics and variability of the atmospheric water balance in the amazon basin: Spatial and temporal variability. Clim. Dyn. 24 https://doi.org/10.1007/s00382-004-0461-6.
Marengo, J.A., Liebmann, B., Kousky, V.E., Filizola, N.P., Wainer, I.C., 2001. Onset and end of the rainy season in the brazilian amazon basin. J. Clim. 14, 833–852. https://doi.org/10.1175/1520-0442(2001)014<0833:OAEOTR>2.0.CO;2.
Martin, S.T., Andreae, M.O., Althausen, D., Artaxo, P., Baars, H., Borrmann, S., Chen, Q., Farmer, D.K., Guenther, A., Gunthe, S.S., et al., 2010. An overview of the amazonian aerosol characterization experiment 2008 (amaze-08). Atmos. Chem. Phys. 10, 11415–11438. https://doi.org/10.5194/acp-10-11415-2010.
Martin, S.T., Artaxo, P., Machado, L.A.T., Manzi, A.O., Souza, R.A.F., Schumacher, C., Wang, J., Andreae, M.O., Barbosa, H.M.J., Fan, J., Fisch, G., Goldstein, A.H., Guenther, A., Jimenez, J.L., Pöschl, U., Dias, M.A.S., Smith, J.N., Wendisch, M., 2016. Introduction: Observations and modeling of the green ocean amazon (GoAmazon2014/5). Atmos. Chem. Phys. 16, 4785–4797. https://doi.org/10.5194/acp-16-4785-2016.
Matos, A.P.D., Cohen, J.C.P., 2016. Circulação de brisa e a banda de precipitação na margem leste da baa de marajó. Ciência e Nat. 38, 21–27. https://doi.org/10.5902/2179460X19814.
Medeiros, A.S.S., Calderaro, G., Guimarães, P.C., Magalhaes, M.R., Morais, M.V.B., Rafee, S.A.A., Ribeiro, I.O., Andreoli, R.V., Martins, J.A., Martins, L.D., Martin, S.T., Souza, R.A.F., 2017. Power plant fuel switching and air quality in a tropical, forested environment. Atmos. Chem. Phys. 17, 8987–8998. https://doi.org/10.5194/acp-17-8987-2017.
Melo, A.M., Dias-Junior, C.Q., Cohen, J.C., Sá, L.D., Cattanio, J.H., Kuhn, P.A., 2019. Ozone transport and thermodynamics during the passage of squall line in central amazon. Atmos. Environ. 206, 132–143. https://doi.org/10.1016/j.atmosenv.2019.02.018.
Monteiro, A., Gama, C., Cândido, M., Ribeiro, I., Carvalho, D., Lopes, M., 2016. Investigating ozone high levels and the role of sea breeze on its transport. Atmos. Pollut. Res. 7, 339–347. https://doi.org/10.1016/j.apr.2015.10.013.
Moraes, E.T., Dias-Júnior, C.Q., Cohen, J.C., Corrêa, P.B., Martins, H.S., D'Oliveira, F.A., Kuhn, P.A., Cattanio, J.H., Souza, E.B., de Araújo, A.C., et al., 2022. Simulation of an orographic gravity wave above the amazon rainforest and its influence on gases transport near the surface. Atmos. Res. 278, 106349. https://doi.org/10.1016/j.atmosres.2022.106349.
Nuvolone, D., Petri, D., Voller, F., 2018. The effects of ozone on human health. Environ. Sci. Pollut. Res. 25, 8074–8088. https://doi.org/10.1007/s11356-017-9239-3.
Pacifico, F., Folberth, G., Sitch, S., Haywood, J., Rizzo, L., Malavelle, F., Artaxo, P., 2015. Biomass burning related ozone damage on vegetation over the amazon forest: a model sensitivity study. Atmos. Chem. Phys. 15, 2791–2804. https://doi.org/10.5194/acp-15-2791-2015.
Parrish, D.D., Fehsenfeld, F.C., 2000. Methods for gas-phase measurements of ozone, ozone precursors and aerosol precursors. Atmos. Environ. 34, 1921–1957. https://doi.org/10.1016/S1352-2310(99)00454-9.
Pereira Oliveira, A., Fitzjarrald, D.R., 1993. The amazon river breeze and the local boundary layer: I. observations. Bound.-Layer Meteorol. 63, 141–162. https://doi.org/10.1007/BF00705380.
Planchon, O., Damato, F., Dubreuil, V., Gouéry, P., 2006. A method of identifying and locating sea-breeze fronts in North-Eastern Brazil by remote sensing. Meteorol. Appl. 13, 225–234. https://doi.org/10.1017/S1350482706002283.
Rafee, S.A.A., Martins, L.D., Kawashima, A.B., Almeida, D.S., Morais, M.V.B., Souza, R.V.A., Oliveira, M.B.L., Souza, R.A.F., Medeiros, A.S.S., Urbina, V., Freitas, E.D., Martin, S.T., Martins, J.A., 2017. Contributions of mobile, stationary and biogenic sources to air pollution in the amazon rainforest: a numerical study with the WRF-chem model. Atmos. Chem. Phys. 17, 7977–7995. https://doi.org/10.1590/0102-778620130058.
Ryerson, T., Trainer, M., Holloway, J., Parrish, D., Huey, L., Sueper, D., Frost, G., Donnelly, S., Schauffler, S., Atlas, E., et al., 2001. Observations of ozone formation in power plant plumes and implications for ozone control strategies. Science 292, 719–723. https://doi.org/10.1126/science.1058113.
Saad, S.I., Da Rocha, H.R., Silva Dias, M.A., Rosolem, R., 2010. Can the deforestation breeze change the rainfall in Amazonia? A case study for the br-163 highway region. Earth Interact. 14, 1–25. https://doi.org/10.1175/2010EI351.1.
Santos, M.J., Silva Dias, M.A., Freitas, E.D., 2014. Influence of local circulations on wind, moisture, and precipitation close to Manaus city, amazon region, Brazil. J. Geophys. Res. Atmos. 119, 13–233. https://doi.org/10.1002/2014JD021969.
Santos, Y.L.F.D., Souza, R.A.F.D., Souza, J.M.D., Andreoli, R.V., Kayano, M.T., Ribeiro, I.O., Guimarães, P.C., 2017. Variabilidade espaço-temporal do monóxido de carbono sobre a américa do sul a partir de dados de satélite de 2003 a 2012. Rev. Brasil. Meteorol. 32, 89–98. https://doi.org/10.1590/0102-778632120150163.
Sarangapani, R., Gentry, P.R., Covington, T.R., Teeguarden, J.G., Clewell Iii, H.J., 2003. Evaluation of the potential impact of age-and gender-specific lung morphology and ventilation rate on the dosimetry of vapors. Inhal. Toxicol. 15, 987–1016. https://doi.org/10.1080/08958370390226350.
Shrivastava, M., Andreae, M.O., Artaxo, P., Barbosa, H.M., Berg, L.K., Brito, J., Ching, J., Easter, R.C., Fan, J., Fast, J.D., et al., 2019. Urban pollution greatly enhances formation of natural aerosols over the amazon rainforest. Nat. Commun. 10, 1046. https://doi.org/10.1038/s41467-019-08909-4.
Shukla, J., Nobre, C., Sellers, P., 1990. Amazon deforestation and climate change. Science 247, 1322–1325. https://doi.org/10.1126/science.247.4948.1322.
Silva Dias, M.A.F.D., Silva Dias, P.L.D., Longo, M., Fitzjarrald, D.R., Denning, A.S., 2004. River breeze circulation in eastern Amazonia: observations and modelling results. Theor. Appl. Climatol. 78, 111–121. https://doi.org/10.1007/s00704-004-0047-6.
Silveira, M.V., Silva-Junior, C.H., Anderson, L.O., Aragão, L.E., 2022. Amazon fires in the 21st century: the year of 2020 in evidence. Glob. Ecol. Biogeogr. 31, 2026–2040. https://doi.org/10.1111/geb.13577.
SUFRAMA, 2022. Indústria. <https://www.gov.br/suframa/pt-br/zfm/industria>. Accessed 02.04.22.
Torres, O., Chen, Z., Jethva, H., Ahn, C., Freitas, S., Bhartia, P., 2010. Omi and modis observations of the anomalous 2008–2009 southern hemisphere biomass burning seasons. Atmos. Chem. Phys. 10, 3505–3513. https://doi.org/10.5194/acp-10-3505-2010.
Townsend, C., Maynard, R.L., 2002. Effects on health of prolonged exposure to low concentrations of carbon monoxide. Occup. Environ. Med. 59, 708–711. https://doi.org/10.1136/oem.59.10.708.
Trebs, I., Mayol-Bracero, O.L., Pauliquevis, T., Kuhn, U., Sander, R., Ganzeveld, L., Meixner, F.X., Kesselmeier, J., Artaxo, P., Andreae, M.O., 2012. Impact of the Manaus urban plume on trace gas mixing ratios near the surface in the amazon basin: Implications for the no-no2-o3 photostationary state and peroxy radical levels. J. Geophys. Res. Atmos. 117 https://doi.org/10.1029/2011JD016386.
Vasconcelos, S.S.D., Fearnside, P.M., Graça, P.M.L.D.A., Silva, P.R.T.D., Dias, D.V., 2015. Suscetibilidade da vegetação ao fogo no sul do amazonas sob condições meteorológicas atpicas durante a seca de 2005. Rev. Brasil. Meteorol. 30, 134–144. https://doi.org/10.1590/0102-778620140070.
Werth, D., Avissar, R., 2002. The local and global effects of amazon deforestation. J. Geophys. Res.-Atmos. 107 https://doi.org/10.1029/2001JD000717. LBA–55.
Wiedinmyer, C., Akagi, S., Yokelson, R.J., Emmons, L., Al-Saadi, J., Orlando, J., Soja, A., 2011. The fire inventory from ncar (finn): a high resolution global model to estimate the emissions from open burning. Geosci. Model Dev. 4, 625–641. https://doi.org/10.5194/gmd-4-625-2011.
Xu, R., Tie, X., Li, G., Zhao, S., Cao, J., Feng, T., Long, X., 2018. Effect of biomass burning on black carbon (bc) in south asia and tibetan plateau: the analysis of wrf-chem modeling. Sci. Total Environ. 645, 901–912. https://doi.org/10.1016/j.scitotenv.2018.07.165.
Yue, X., Unger, N., 2014. Ozone vegetation damage effects on gross primary productivity in the United States. Atmos. Chem. Phys. 14, 9137–9153. https://doi.org/10.5194/acp-14-9137-2014.
Yue, X., Unger, N., 2018. Fire air pollution reduces global terrestrial productivity. Nat. Commun. 9, 5413. https://doi.org/10.1038/s41467-018-07921-4.
Zhang, J., Wei, Y., Fang, Z., 2019. Ozone pollution: a major health hazard worldwide. Front. Immunol. 10, 2518. https://doi.org/10.3389/fimmu.2019.02518.
Zhao, T., Ye, J., Ribeiro, I.O., Ma, Y., Hung, H.M., Batista, C.E., Stewart, M.P., Guimarães, P.C., Vilà-Guerau de Arellano, J., De Souza, R.A., et al., 2021. River winds and pollutant recirculation near the Manaus city in the central amazon. Commun. Earth Environ. 2, 205. https://doi.org/10.1038/s43247-021-00277-6.
Zhong, S., Leone, J.M., Takle, E.S., 1991. Interaction of the sea breeze with a river breeze in an area of complex coastal heating. Bound.-Layer Meteorol. 56, 101–139. https://doi.org/10.1007/BF00119964.
Zhou, Y., Guan, H., Huang, C., Fan, L., Gharib, S., Batelaan, O., Simmons, C., 2019. Sea breeze cooling capacity and its influencing factors in a coastal city. Build. Environ. 166, 106408. https://doi.org/10.1016/j.buildenv.2019.106408.